Earth Surface Processes and Landforms

Reach-scale bankfull channel types can exist independently of catchment hydrology

Journal:	*Earth Surface Processes and Landforms*
Manuscript ID	ESP-19-0231.R1
Wiley - Manuscript type:	Research Article
Date Submitted by the Author:	n/a

Complete List of Authors:	Byrne, Colin; University of California Davis, Land, Air and Water Resources Pasternack, Gregory; University of California Davis, Land, Air and Water Resources Guillon, Hervé; University of California Davis, Land, Air and Water Resources Lane, Belize; Utah State University, Department of Civil and Environmental Engineering Sandoval-Solis, Samuel; University of California Davis, Land, Air and Water Resources

Keywords:	channel-reach morphology, multivariate classification, hydrogeomorphic, hydraulic geometry, basin hydrology

Reach-scale bankfull channel types can exist independently of catchment hydrology

Author names:

Colin F. Byrne[1], Department of Land, Air & Water Resources, One Shields Ave., Davis, CA 95616; cfbyrne@ucdavis.edu

Gregory B. Pasternack[1]

Hervé Guillon[1]

Belize A. Lane[2]

Samuel Sandoval-Solis[1]

Author affiliations:

[1]University of California Davis, Department of Land, Air & Water Resources

[2]Utah State University, Civil and Environmental Engineering

Abstract

Reach-scale morphological channel classifications are underpinned by the theory that each channel type is related to an assemblage of reach- and catchment-scale hydrological, topographic, and sediment supply drivers. However, the relative importance of each driver on reach morphology is unclear, as is the possibility that different driver assemblages yield the same reach morphology. Reach-scale classifications have never needed to be predicated on hydrology, yet hydrology controls discharge and thus sediment transport capacity. Scientifically, the novel question is whether two or more regions with different hydrological settings end up with different reach-scale channel types or if channel types may universally transcend hydrological settings because hydrology is not a primary control at the reach scale. This study answered this question by isolating hydrology as a potential driver of channel type. Three methods were employed within a large test basin with diverse hydrological settings (Sacramento River, California): (1) creation of a reach-scale channel classification based on local site surveys, (2) binning of stream sites by annual hydrologic regime, flood magnitude, and dimensionless flood magnitude, and (3) statistical assessment of two hydrogeomorphic linkages: the spatial distribution of channel types across hydrological settings and the dependence of channel type morphological attributes on defining hydrology. Results yielded ten channel types; nearly all types existed in nearly all hydrological settings, which is perhaps a surprising development for hydrogeomorphology. Downstream hydraulic geometry relationships were statistically significant. In addition, cobble-dominated uniform streams showed a consistent inverse relationship between slope and dimensionless flood magnitude, an indication of dynamic equilibrium between transport capacity and sediment supply. However, most morphological attributes showed no sorting by hydrological setting. This study suggests that median hydraulic geometry relations persist across basins and within channel types, but hydrological influence on geomorphic variability is likely due to local influences rather than catchment-scale drivers.

Keywords: channel-reach morphology, multivariate classification, hydrogeomorphic, hydraulic geometry, basin hydrology

1. Introduction

1.1. The importance of reach-scale morphological classification

Classification of reach-scale morphology is critical for integrated river basin management (Gurnell et al., 2016; Kondolf et al., 2016). Reach-scale morphology and associated processes are indicative of ecohydraulic differences (Lane et al., 2018a) that control ecologically significant biogeochemical processes and species habitat (Dahm et al., 1998; Moir and Pasternack, 2010). Here, we use the term reach-scale morphology to describe streams with similar valley, cross-sectional, planform, longitudinal bedform, and sediment characteristics at scales of approximately 10 – 20 channel widths, or more simply, streams comprised of similar morphological units in similar valley settings (Frissell et al., 1986; Wyrick and Pasternack, 2014).

Reach-scale classifications seek to organize complex morphologies and processes occurring across a landscape. Although classifications have been conducted for a variety of purposes (see Kondolf et al., 2016 for review), both a universal classification and a universal methodology towards classification have yet to be firmly established. The lack of consistency in classification methodologies likely stems from the fact that rivers are complex across multiple scales. Reach-scale morphology represents a mesoscale in which smaller geomorphic units are integrated and larger channel segment and basin processes must be represented by a given smaller form (Frissell et al., 1986). Classifications that focus on measured channel attributes capture sub-reach scale morphological features and hydraulic conditions, such as pool formation by flow-convergence routing or secondary flow dynamics (MacWilliams et al., 2006; Thompson, 1986). Classifications attempting to correlate reach-scale morphology with reach-, segment-, or basin-scale processes using remotely-sensed channel slope, valley confinement, and drainage area apply a process domain concept to represent morphology across scales (Church, 2002; Flores et al., 2006; Montgomery, 1999; Polvi et al., 2011; Wohl, 2010). In addition to the multi-scale processes influencing reach-scale morphology, classifications are static representations of dynamic systems (Lane, 1995). Although reach-scale morphology (e.g. step-pool, riffle-pool) may remain constant through time, sub-reach scale characteristics are fundamentally within an erosional or depositional cycle and subject to both gradual and nearly instantaneous complex changes (Schumm, 1977). Since only the largest sediment clasts will remain immobile during large flood events and entrainment of various sediment sizes occurs under different flow conditions (Miller et al., 1977; Shields, 1936), a relationship may develop between reach-scale morphology and hydrological disturbance.

1.2. The influence of hydrology on reach-scale morphology

The literature generally presents classified reach-scale morphologies as a product of catchment hydrology, sediment delivery, and topography, which in turn are governed by tectonics, lithology, and climate; however, the relative influence of each on reach-scale morphology is often unclear. Attempts to relate reach-scale morphology to local hydrology and streamflow patterns stem from established fundamental downstream relationships between discharge magnitude and channel hydraulic geometry (Leopold and Maddock, 1953; Richards, 1977). Discharge magnitude has been combined with slope to represent both hydrological and landscape influences on transport capacity when defining channel planform (Leopold and Wolman, 1957). Inclusion of a discharge metric or correlated surrogate (e.g. contributing area) is also fundamental to many process domain classifications (Church, 2002; Flores et al., 2006; Polvi et al., 2011). These classifications have been shown to improve predictive power when a hydrological-based metric representative of transport capacity is included (Flores et al., 2006), as compared to previous slope-based classifications established by Grant et al. (1990) and Montgomery and Buffington (1997).

Leopold and Wolman (1957) noted the related nature of channel cross-section geometry, planform, longitudinal form, and sediment characteristics. A reach-scale classification aims to encapsulate all of these variable dimensions of form, which leads to clear reasoning for the inclusion of a discharge metric in classification methodologies. However, the use of discharge-slope thresholds to define river pattern has been challenged, and evidence suggests that channel geometry, planform, and reach-scale morphology are more closely related to sediment supply and grain size characteristics (Carson, 1984; Church, 2006; Friend, 1993; Harvey, 1991; Pfeiffer et al., 2017). Due to hierarchical river patterns and topographic variability, it is not surprising that both hydrology and sediment supply are controls on reach-scale morphology, but to what degree is unclear.

116 Beyond studies that relate individual channel attributes or reach-scale morphology to local discharge or transport capacity metrics, there is a broader conceptualization that regions can be characterized by distinct hydrological regimes. A hydrological regime is defined by the magnitude, frequency, duration, rate of change, and timing of streamflow conditions over a period of interest (Poff et al., 1997). Many studies have classified hydrological regimes in different regions of the world (Bard et al., 2015; Beechie et al., 2006; Lane et al., 2017a; Thanapakpawin et al., 2007; Yang et al., 2002). However, in contrast with the literature linking channel metrics to local flow magnitude, no studies have demonstrated a link between an overall hydrological regime and a set of regime-adjusted channel types within a region, let alone variances between channel typologies and hydrological regimes within a region. Pfieffer and Finnegan (2018) note that continental differences in the mobilization of gravel-bed stream sediments, fundamental to the formation of bedforms, occur first due to sediment supply and second due to differences in hydrology. Whether these findings result in distinct reach-scale morphologies or are minutia is unknown. In a more dichotomous, global comparison of hydrological differences in channel form, arid and humid landscapes exhibit differences in channel attributes and sensitivity to hydrological disturbances (Graf, 1988; Reid and Laronne, 1995; Tooth, 2000). At a regional scale, however, it is unclear, for instance, whether a snowmelt-dominated hydrological regime would yield different reach-scale channel types than a rain-dominated regime.

137 Despite some support in the literature for hydrologic controls on reach-scale morphology, complexity in the formation of channel types at the local scale complicates

these relationships. Local topographic control and geomorphic processes are important controls on reach-scale morphology through their controls on integrated local processes. Bedrock, large wood, vegetation, and bioengineered structures are often observed to influence reach-scale morphology by forcing the occurrence of various morphological units (Bisson et al., 1996; Buffington et al., 2002; Fryirs and Brierley, 2012; Montgomery et al., 1996; Wohl, 2013). If a reach is subjected to continual local disturbances or topographic drivers, such as those occurring in a heavily vegetated and confined setting, sub-basin hydrology is less likely to influence reach-scale morphology. Whether or not basin hydrology exerts defining controls over local processes is unclear.

1.3. Defining the scientific question

In conjunction with complexity exerted from local geomorphic influences, there is also ample evidence that similar reach-scale morphologies exist across a range of arid to humid hydrological settings (Chin and Wohl, 2005; Makaske, 2001; Montgomery and Buffington, 1997; Sutfin et al., 2014). An argument for the limited control of hydrology on reach-scale morphology may be inferred from Hack (1960), who postulated that rivers have many mutually adjustable variables operating via many mechanisms of fluvial adjustment. That concept can be applied to this problem to hypothesize that a shift or difference in any one variable (such as hydrological regime or flood magnitude) may simply be adjusted away by something else without necessitating a shift or difference in channel type. This logic suggests that topographic controls and local geomorphic influences are more important than hydrological setting in determining reach-scale morphology. Alternately, it may be that reach-scale morphology is determined predominately by the minimum energy principle. In this case, a difference in hydrological setting may not change the fundamental need for a particular reach-scale morphology to be present in order to satisfy a number of documented extremal conditions such as minimum hydraulic dimension variance, minimum energy dissipation rate, minimum stream power, or maximum friction factor (Chang, 1979; Davies and Sutherland, 1983; Huang et al., 2004; Langbein and Leopold, 1964; Yang et al., 1981). To what extent is hydrology a dominant control on reach-scale morphology, or is reach-scale morphology largely independent of hydrological setting because other topographic and local characteristics exert stronger controls? Although the answer may depend on the scale of hydrological variability, the question is important to address for more complete understanding of controls on reach-scale morphology. We sought to answer the presented scientific question with a novel experimental design, presented immediately below, followed by more specific methodologies in Sections 4 and 5.

2. Experimental design

In this study, we explicitly investigated the relationship between hydrological setting and reach-scale morphology within a river basin. Here, the term hydrological setting is defined as gauge-extrapolated annual hydrological regime or flood magnitude characteristics. The hydrological setting is defined at a sub-basin scale. Three hydrological binning methodologies were analyzed in conjunction with reach-scale morphology to answer a series of specific questions: (1) are *annual flow regimes* indicative of reach-scale morphology, (2) are *flood magnitudes* indicative of reach-scale morphology, and (3) are *dimensionless flood magnitudes* indicative of reach-scale morphology? For each hydrological binning method and associated question, geomorphic metrics used to represent reach-scale morphology include categorical classified reach-scale morphologies (e.g., pool-riffle), henceforth called channel types, and common field-measured channel attributes (e.g., bankfull depth) of each channel type. Statistical bootstrapping and nonparametric Kruskal-Wallis tests were used to quantitatively assess the uncertainty of hydrological-geomorphic relationships. The experimental design is conceptualized in Figure 1 and more specific methodologies are explained in Section 4.

Given more channel types than hydrological settings, we expected that some channel types would exist across multiple hydrological settings while others would be unique to specific hydrological settings. Within channel types, we expected streams subjected to different hydrological settings to display significant differences in the values of associated geomorphic attributes due to differences in hydrology and related hydraulic processes. For example, a steep mountain stream may predominantly exist in small flood magnitude systems because larger flood magnitude systems are generally associated with lower gradient, high order streams. Alternatively, the annual flow regime may not be an effective indicator of mountain stream locations, as flow regimes in mountainous channel settings may include a range of rain to snowmelt influence. The annual flow regime may be a more significant hydrological control on channel types in other settings, such as along an arid - temperate gradient where vegetative and bank sediments may drive differences in channel patterns (e.g., braided or single thread) and dimensionality. Thus, more broadly, we hypothesized that hydrological settings will control the sub-basin variability and spatial distribution of channel types, although the dominance of this control will depend on the specific channel type.

3. Test basin

The Sacramento River basin is the second largest river by volume draining to the Pacific Ocean in the continental United States, making it suitably large and hydrogeomorphically diverse to serve as the testbed for this study (Palmer, 2012). The basin covers approximately 70,000 km^2, predominantly within California with the northernmost headwaters extending into Oregon (Fig. 2). For context, the Sacramento River basin is comparable to the Yodo (Japan), Kizilirmak (Turkey), and Seine (France) rivers, and estimated to be one of the largest 200 rivers draining directly to an ocean (Milliman and Syvitski, 1992). The basin is geologically complex with multiple physiographic provinces represented, including the Coastal range to the west, the southern Cascade Range, the Sierra Nevada, the volcanic uplands of the Modoc Plateau, and the basin and range province in northeastern California. The Sacramento River flows roughly north to south through the Central Valley of California and combines with the San Joaquin River to form the Sacramento-San Joaquin River Delta, which ultimately drains into the Pacific Ocean.

The Sacramento River basin exhibits order-of-magnitude differences in mean annual precipitation, with approximately 28 cm in the northeastern high plateau and basin and range settings to over 275 cm in the northern Sierra Nevada (PRISM Climate Group, 2007). The basin is subjected to a Mediterranean climate with cool, wet winters and warm, dry summers. The seasonality and inter-annual variability of storm events plays a large role in the spatiotemporal distribution of flow regimes across the state, while topographic and geologic variability add further complexity. Within the basin, portions of the Coastal Range and Sierra Nevada can be subjected to similar major winter storm events, but differences in elevation and topographic orientation drive strong differences in hydrological regime (Lane et al., 2017a).

In addition to the complex physiographic and climatic conditions across the basin, streams within the Sacramento River basin have been subjected to a plethora of human-induced hydrogeomorphic alterations over the past two hundred years. Perhaps the most well documented and glaring human-induced fluvial changes were due to hydraulic mining within the basin, of which the impacts are ongoing (Gilbert, 1917; James, 1991; White et al., 2010). Hydrologically, at least 435 dams have been built within the basin, which will impact the hydrogeomorphology of the streams locally, at the very least, and in some cases have lingering impacts to the entire basin (Kondolf, 1997; Singer, 2007). Heavy agricultural and urban development has dominated within the Central Valley of the Sacramento River basin and other land use practices include but are not limited to logging, gravel pit mining, and animal grazing (Mount, 1995). All of these changes are important to keep in mind when examining hydrogeomorphic relationships throughout the basin.

4. Reach-scale morphological classification methodology

A multivariate data-driven statistical approach to reach-scale classification was used in this study to avoid preconceived channel type descriptions and is similar to other statistical classifications (e.g. Sutfin et al. (2014) or Kasprak et al. (2016)). Twelve geomorphic attributes were considered for the reach-scale classification. Nine geomorphic attributes were calculated from field surveys: water surface slope (s), bankfull depth (d), bankfull width (w), bankfull width-to-depth ratio (w/d), coefficient of variation of bankfull depth (CV_d), coefficient of variation of bankfull width (CV_w), median grain size (D_{50}), 84th percentile grain size (D_{84}), and channel roughness (d/D_{50}). Three additional geomorphic attributes were estimated using geographic information system (GIS) techniques: hydrological contributing area (A_c), sinuosity (k), valley confinement distance (C_v). Although subject to limitations (Kondolf et al., 2016), stream classification using channel measurements and 10-m resolution, remote-sensed, land surface attribute rasters, as was used in this paper, remains the most achievable strategy; 1-m resolution data are often unavailable (especially for bathymetry), too computationally intensive for basin-wide analysis, or not optimal for direct measurement based on a lack of bathymetry data.

4.1. Site selection

In this study, a stratified statistical sampling design was used to select a reasonable number of representative sites to characterize variability in fluvial geomorphic settings across the landscape. A total of 288 wadeable stream reaches were selected for surveying out of ~119,000 possible 200-m reaches basin-wide. Of these, 139 reaches were surveyed by the University of California-Davis (UCD) and 149 reaches by the California State Water Resources Board's Surface Water Ambient Monitoring Program (SWAMP) (Fig. 2). Because the study focused on wadeable streams of 2nd or larger Strahler-order, over 90% of survey sites were on 2nd to 4th order streams. In addition, over 90% of sites were located in one of the six mountainous Level III ecoregions that make up the basin (Omernik, 1987).

In relation to anthropogenic impacts within the basin, 88% of the surveyed sites are classified as free flowing rivers (Grill et al., 2019), although impacts to low order streams may not always be appropriately represented in this number (Grill et al., 2019). The numerous stream reaches in the basin with large upstream storage dams that have been documented to substantially alter hydrology were not the focus of this study (Singer, 2007). The land use of survey sites can be summarized as 70% forest and woodland, 13% developed and other human use, 10% shrub and herb vegetation, 5% agricultural and developed vegetation, and 3% desert and semi-desert (USGS, 2016). Of the developed sites, 76% exist within open space while the remaining 24% exist in low or medium development (USGS, 2016). Sites that showed clear evidence of human engineering were not included in this analysis. Due to the fact that the majority of these sites exist within mountainous, forested sites, we expect that mining, logging, or grazing would impose the most relative hydrogeomorphic changes to these sites. However, there has been ample decades and sufficient flooding for Hack's (1960) "quick" natural geomorphic adjustments to such anthropogenic impacts. This means that any overarching hydrological control on channel type should be able to handle such mountain-setting anthropogenic dynamics and shine through in the data. Selecting sites with a stratified sampling approach ideally normalizes the anthropogenic impacts across all sites.

Field survey site locations were determined using an equal effort stratified random sampling scheme based on GIS-desktop-computed slope and contributing area values, as documented in Lane et al. (2017b). Slope categories, based on Rosgen (1994) as a classification comparison, were defined as <0.1%, 0.1-2%, 2-4%, 4-10%, and >10%. Contributing area categories differed based on physiographic province (i.e. Pacific Border or Cascade-Sierra Nevada) due to the assumption that differences in climate, topography, and lithology would drive differences in transport capacity under similar contributing area settings (Lane et al., 2017b). Pacific Border area categories were <50, 50-5,000, and >5,000 km^2, while Cascade-Sierra Nevada sites were <300, 300-9,000, and >9,000 km^2. The slope - area sampling protocol was designed to capture variability in transport capacity. Since some slope – area bins were expected to be more prevalent on the landscape than others (e.g. a stream of a given Strahler order are approximately twice as common as a stream of one higher order), an equal number of reaches was surveyed in each bin to ensure that all channel settings including rare channel types are represented in the classification. The slopes used for site selection were not used in the geomorphic classification.

A GIS, ESRI ArcGIS 10.4 (ESRI, 2016), was used for geospatial analysis to select specific survey locations. Contributing area was calculated based on the United States Geological Survey (USGS) 10-m National Elevation Dataset (NED) and streamlines defined by the National Hydrography Dataset (NHD) version 2 (Gesch et al., 2002; McKay et al., 2012). Slope was estimated from the 10-m DEM as the change in elevation along the reach divided by the reach length. This technique provides a desktop estimate of slope but is susceptible to error, especially for short stream segments (Neeson et al., 2008). For this reason, slope was re-calculated from survey measurements for use in subsequent geomorphic statistical analysis. GIS desktop slope computation only aided site selection, nothing more.

4.2. Site surveys and data processing

Field surveys were completed by UCD survey teams in summers of 2015 through 2017. Survey methodologies were based on SWAMP protocols to enable comparability between datasets (Ode, 2007). At each site, average bankfull width was estimated to determine the reach survey length. Survey lengths were 150 or 250 m for streams with average wetted widths less than or greater than 10 m, respectively. This produced stream reaches with a median length of 18.8 channel widths. Eleven equally spaced cross-sectional transects along the reach were surveyed using rod and level techniques. Bankfull depth was defined using geomorphic and vegetative indices as defined by Ode (2007) for SWAMP protocols, including slope breaks, change from annual to perennial vegetation, and changes in sediment size. Bankfull depth and water depth were recorded at the thalweg. A Wolman pebble count was conducted at each transect (Wolman, 1954), and a longitudinal survey was conducted along the thalweg at each cross-section.

Mean values of bankfull width, depth, and bankfull width-to-depth ratio were calculated as the mean of all survey transect measurements. In addition, 50th and 84th percentile grain sizes were calculated over the entirety of each reach. If the channel was split within the survey length, bankfull depth was calculated as the mean of each split channel at a given transect and bankfull width was calculated as the sum of each split channel width. Width-to-depth of split channels at a transect was calculated as the average width-to-depth of each individual channel. Reach slope was calculated from the best-fit regression line of surveyed water surface elevations along the thalweg. The roughness parameter was calculated as the ratio of bankfull depth to median grain size. Within-reach coefficients of variation of bankfull width and bankfull depth were calculated as the ratio of standard deviation to mean attribute values across the surveyed transects. Here, coefficients of variation of width and depth are referred to as topographic variability attributes (TVAs). Lane et al. (2017b) previously documented that TVAs displayed considerable importance in the identification of distinct channel types.

4.3. Desktop geospatial data collection for multivariate channel classification

A GIS was also used for geospatial analysis in the estimation of certain channel and valley attributes used in statistical analysis. The same values of contributing area that were used in site selection were also used in site classification (see 4.1). Sinuosity has been used as a defining metric in previous classifications (Rosgen, 1994) and was calculated as the ratio of channel thalweg length to distance between upstream and downstream vertices within the GIS. Stream channels were digitized based upon aerial imagery, digital USGS topographic maps, and NHD layers for 1000 m. Because sinuosity is sensitive to the scale at which it is calculated (Snow, 1989), 1000 m sinuosity was used to represent the channel reach length at approximately 100 times the bankfull width.

Valley setting and confinement play both qualitative and quantitative roles in the majority of previous channel classification methodologies due to the influence of distinct valley setting processes in the creation of characteristic forms (Beechie and Imaki, 2014; Brierley and Fryirs, 2000; Fryirs et al., 2016; O'Brien et al., 2019; Rosgen, 1994). Here, valley widths were delineated using a methodology similar to previous literature (Gilbert et al., 2016; O'Brien et al., 2019). For the purposes of this study, 25 percent slope was chosen as a threshold between valley bottom and valley wall capturing a medial value between clay and sand dominated hill footslopes (Carson, 1972). The 10-m DEM was converted to a slope raster and reclassified. Valley bottom polygons (i.e. areas with less than 25% slope) were created to clip 5,000 m cross-section polylines to site specific lengths. Four cross-sections per 200-m of stream length were averaged to calculate a single valley confinement distance that was subsequently used in the geomorphic classification. Confined, partly-confined, and unconfined valley nomenclature of channel types was defined by a logarithmic scale of <= 100 m, >100 and <= 1000 m, and > 1000 m, respectively.

4.4. Multivariate statistical channel archetyping

Several multivariate statistical techniques were used to identify clusters of field-surveyed geomorphic attributes corresponding with distinct channel types following Lane et al. (2017b). Statistical techniques included non-metric multidimensional scaling (NMDS) (Anderson, 2001; Clarke, 1993; Kruskal, 1964), principal component analysis (PCA), hierarchical clustering using Ward's algorithm (Ward's hierarchical clustering; WHC) (Murtagh and Legendre, 2014a, 2014b; Ward, 1963), classification trees (De'ath and Fabricius, 2000), and the combination of nonparametric Kruskal-Wallis and Wilcoxon Rank Sum Tests (Kabacoff, 2015). The R language was used for all statistical analysis (R Core Team, 2017). Initial correlations were conducted by calculating Pearson's correlation coefficient for rescaled attribute values ('cor' function, stats package). All channel attributes were rescaled from zero to one for multivariate approaches. NMDS was conducted using the metaMDS function (vegan package) (Oksanen et al., 2019), and PCA used the 'prcomp' function (stats package). The WHC utilized the 'hclust' function with the method defined as 'Ward.D2' (stats package) and the 'NbClust' function to assess the suggested number of hierarchical clusters (NbClust package) (Murtagh and Legendre, 2014a). The classification tree approach was conducted with the 'rpart' function, run using a classify approach, and pruned with the 'prune' function (rpart package) (Therneau and Atkinson, 2018). Finally, Kruskal-Wallis and Wilcoxon Rank Sum Tests were conducted using the 'oneway' function (npar package) (Kabacoff, 2015).

The following four steps were implemented to determine the final geomorphic classification. First, linear regressions between all geomorphic attributes were conducted and attributes with absolute values of the correlation coefficient greater than 0.7 were removed. The remaining geomorphic attributes were rescaled from zero to one to provide equal weight to each. Second, calculation of the minimum stress value produced by NMDS, in combination with principal component vectors, allowed for comparison between attributes and plotting of multi-dimensional clusters in two-dimensional space. Third, the data were stratified using WHC, which minimizes within-cluster variance and maximizes between-cluster variance. Ideally, more similar channel types will cluster together. The Hubert Index was used to inform selection of an appropriate number of channel types. Heuristic refinement of statistical clusters was conducted based on field reconnaissance and expert knowledge of specific field sites. The goal, similar to all classifications, was to balance regional stream heterogeneity with a measure of simplification. While statistics drove the initial classification, heuristic comparison of site-specific features was used to refine channel types. Fourth, because branches within the hierarchical clustering do not necessarily have physical meaning, a classification tree supplemented WHC by assessing the ability of geomorphic attributes to correctly define channel types. Channel types, as defined by the heuristic-WHC methodology, were used as the prediction groups for the classification tree leading to a percentage of site being classified accurately. Given a distinct number of channel types, pruning of the classification tree was conducted to optimize cross-validation accuracy between classification tree predictions and heuristic-WHC channel types. Here, classification trees represent a diagnostic tool and interpretable technique to understand the stability of the multivariate clustering and cross-validation accuracy, included in the approach presented here, is a measure of the model to generalize to unseen data. Kruskal-Wallis and Wilcoxon Rank Sum Tests also allowed for the comparison of attribute distributions across channel types.

5. Hydrological binning methods to assess hydrogeomorphic questions

5.1. Are *annual hydrological regimes* indicative of reach-scale morphology?

A previously established hydrological stream classification within California defines key characteristics of the dominant annual flood hydrograph related to timing, magnitude, duration, frequency, and rate of change characteristics at a given location (Lane et al., 2018b). Lane et al. (2018b) classified stream gauges in California based on a variety of hydrological indices (e.g. mean annual flow, date of minimum/maximum flow, small/large flood frequency, etc.) and extrapolated those attributes using topographic, geologic, and climatic conditions to define annual hydrological regimes to ungauged streams (Lane et al., 2017a). Annual hydrological regimes were directly attributed to reach-scale survey sites in this study using the NHD stream network. Five annual hydrological regimes were represented by the 288 surveyed channel reach locations included High elevation and Low Precipitation (HLP) (n = 25), Low-volume Snowmelt and Rain (LSR) (n = 120), Perennial Groundwater and Rain (PGR) (n = 54), Rain and seasonal Groundwater (RGW) (n = 51), and Winter Storms (WS) (n = 38) (Table 1, Fig. 3a).

5.2. Are *flood magnitudes* indicative of reach-scale morphology?

Because differences in hydrological regime do not necessarily translate to differences in disturbance regime (Poff et al., 2006), flood magnitude was used to assess the magnitude of hydrological disturbance at a given site. Flood magnitudes for the Sacramento River basin were collected from a previous USGS flood-frequency analysis of gauges with a minimum of 30 years of unregulated flow (Parrett et al., 2011). Only gauge locations along streamlines defined by the five previously described Lane et al. (2018b) annual hydrological regimes were used, which resulted in USGS flood-frequency estimates at 84 locations. Contributing area-discharge regressions were generated for each of the annual hydrological regimes based on gauge records (see Supplementary Information). Flood magnitudes of 2-, 5-, 10-, 25-, and 50-year recurrence intervals were calculated from the regressions at each of the channel survey sites. Ultimately, 10-year recurrence interval floods were considered here as the number of statistically significant bootstrapping results, which are described in more detail below, were near maximum and maximum for flood magnitude and subsequent dimensionless flood magnitude analysis below, respectively. The 10-year recurrence interval has physical importance as well, because California has experienced an approximately decadal flood recurrence cyclicity over its measured and longer anecdotally recorded history (Guinn, 1890). Such a consistent disturbance regime could be expected to imprint on channel type if hydrology is a dominant control. In addition, significant within channel type returns were comparable to the 50-year return period, which maximized statistical significance in channel attributes. Use of the results that maximized statistically significant returns would therefore provide the strongest indication of hydrological influence on reach-scale morphology. In contrast to the categorical annual hydrological regime settings which were predetermined, continuous-value flood magnitudes needed to be grouped for statistical bootstrapping of hydrological settings. Therefore, flood magnitude sites were binned into terciles (<33%, 33-66%, >66%), effectively defining sites as having low, medium, or high flood magnitudes (Fig. 3b) as well as ten quantiles to equal the number of channel types. The two approaches were conducted to account for different results in the statistical bootstrapping approach, per Section 5.4.

5.3. Are *dimensionless flood magnitudes* indicative of reach-scale morphology?

Because a given flood magnitude is expected to have different impacts in channels of varying geometry and grain size, flood magnitude was scaled by specific geomorphic attributes to ascertain a dimensionless relative disturbance value. Dimensionless flood magnitudes were calculated by non-dimensionalizing discharges calculated in the flood magnitude analysis by median grain size (D_{50}) and bankfull width (w). Dimensionless discharge was previously defined by Parker et al. (1979) and Pitlick and Cress (2002) (Eqn. 1).

$$\tilde{Q} = {}^{Q}/\left(\sqrt{RgD_{50}} * D_{50}{}^{2}\right) \qquad \text{(Eqn. 1)}$$

Here R is the submerged specific gravity of sediment assumed to be 1.65 and g is the acceleration due to gravity. The equation was adapted for this study to account for channel dimensions (bankfull width, w) in addition to D_{50} with the interest of understanding the relative magnitude of a defining flood in relation to channel dimensions and roughness elements (Eqn. 2).

$$\tilde{Q} = {}^{Q}/\left(\sqrt{RgD_{50}} * w^{2}\right) \qquad \text{(Eqn. 2)}$$

Sites were grouped into hydrological bins defined by low, medium, or high dimensionless flood magnitude using terciles (Fig. 3c), and also split into ten quantiles similarly to flood magnitude.

5.4. Assessment of hydrological influence on reach-scale morphology

Prior to statistical analysis of hydrological influence on channel type, multivariate outliers within each channel type were removed. Multivariate outliers are suggestive of forms that differ from the median tendencies of a multivariate cluster. Therefore, they are least representative of a given channel type and not as indicative of relationships between that channel type and hydrology. Mahalanobis distances were used to determine multivariate outliers using the ‘mvoutlier’ package (Filzmoser et al., 2005; Filzmoser and Gschwandtner, 2012) with the chi-squared quantile specified as 97.5% and a proportion of observations used in calculation of the minimum covariance determinant of 0.75.

The geomorphic classification was statistically evaluated with respect to each of the three hydrological binning alternatives. Statistical tests of the hydrogeomorphic relationships were the same for each of the three hydrological binning alternatives. The influence of hydrology on channel type was assessed using: (1) a nonparametric statistical bootstrapping with replacement to understand how channel types are distributed across hydrological settings relative to equal-probability random occurrence, and (2) a nonparametric Kruskal-Wallis test between hydrological settings for each channel attribute in each channel type.

Statistical bootstrapping indicates whether a channel type is more or less likely to occur within a given annual flow regime, flood magnitude, or dimensionless flood magnitude bin relative to equal-probability random occurrence. Bootstrapping was conducted by randomly assigning a hydrological setting to each of the remaining 235 sites after outlier removal. This was repeated 1000 times to obtain robust statistical expectations for how unique the matching between hydrological setting and channel type would be for each channel type given the number of samples in the observational dataset. Two different tests were considered. First, the percent of sites occurring in a specific hydrological setting for each channel type may be computed and compared between real and bootstrapped datasets. In comparing the observed versus bootstrapped results, if the number of sites in a hydrological setting is indistinguishable from random, then there is no indication of hydrological control on channel type. For hydrology to universally control channel type, we propose that > 70% of hydrological settings across all channel types would deviate from a random number of sites with more than 95% confidence. Second, the number of hydrological settings occurring in a channel type was compared against bootstrapped results. Because the number of sites per channel type can be small, there is no guarantee that all settings will be represented in all channel types in the bootstrapped dataset. For hydrology to universally control channel type, then we propose that > 70% of channel types should deviate from the random number of hydrological settings occurring within a channel type. For flood magnitude and dimensionless flood magnitude analyses, three quantiles maximized significance for the number of sites within a hydrological setting for each channel type, while ten quantiles maximized significance for the number of hydrological settings in each channel type. Results are deemed significant if the probability that the number of sites in a hydrological setting for a channel type, or, the number of hydrological settings in a channel type is less than 5% when compared to bootstrapping results.

The Kruskal-Wallis tests were conducted to investigate hydrological influence on geomorphic attributes within each classified channel type between every possible hydrological setting for two groupings of variables we term gross dimensional attributes and feature attributes of each channel type. Slope, bankfull depth, bankfull width, and width-to-depth ratio constitute gross dimensional attributes that the literature expects to have tight linkages with hydrology. Coefficient of variation in bankfull depth, coefficient of variation in bankfull width, sinuosity, D_{50}, and D_{84} are termed feature attributes, because the literature has either not significantly investigated their reach-scale linkages with hydrology or they are considered as secondary adjustable fluvial variables. The ‘kruskal.test’ function (stats package) was used to calculate significance levels. For channel types that only occurred in one hydrological class, this analysis was not possible. Therefore, this analysis resulted in 81 tests for each of the annual hydrological regime, flood magnitude, and dimensionless flood magnitude binning methods. To more simply represent all Kruskal-Wallis tests, the results are presented as a binary plot of statistical significance for each channel attribute in each channel type as seen in the conceptual example of Figure 4. The occurrence of multiple significant returns for a given channel attribute across channel types would therefore indicate that hydrology consistently leads to differences in that channel attribute. We propose that an attribute should show significant differences in > 70% of channel types at the 95% confidence level for hydrology to be deemed a universal control on that attribute. Further investigation into the meaning of significant returns was conducted for channel attributes that showed significance across multiple channel types.

6. Results

6.1. Reach-scale morphological classification

Sediment size and valley confinement were identified as the most influential factors in multivariate clustering. The three-dimensional NMDS solution recorded a stress value of 0.097 with a non-metric coefficient of determination of 0.991 between observed dissimilarity and ordination distance (Fig. 5a). The first and second principle component axes (PCAs) resulting from the NMDS ordination explained 45 and 19% of the variance in the data, respectively. Loadings of 0.94 for D_{84} and 0.91 for C_v for PCA-1 and PCA-2, respectively. These loading values indicate that these two variables had the strongest influence on multivariate clustering compared to other independent variables.

Ten channel types were identified using WHC with heuristic refinement and tested for geomorphic significance and performance with a classification tree analysis (Figs. 5b, 5c, and 6). The Hubert Index suggested three Ward's clusters as the optimal number of groupings driven by strong breaks in sediment size and valley confinement. As three groups was insufficient to describe the variability of reach-scale morphology within the basin, secondary indications by Hubert Index values at 10 and 14 groups were the focus of heuristic refinement. The final ten channel types were the result of a heuristic dissolution and aggregation of the WHC dendrogram including the combination of splits in clusters 3 and 7, which outperformed combination with channel types 1 and 10, respectively, under classification tree analysis. Physical similarity between combined clusters was confirmed based on analysis of site photography. The classification tree produced a successful classification rate of 84%. Ten-fold cross-validation prediction percentage, which represents the accuracy of a decision tree model when applied to a subset of data not used in tree creation, of this classification tree was 75%. Further statistical analysis addressing the performance of the classification presented here on unseen data can be found in the Supplementary Information.

Final channel types were made up of 6 to 45 sites. Clusters with a small number of sites were avoided, as outliers were expected to represent site-specific differences rather than larger basin trends. However, it was ultimately the uniqueness of cluster attributes that drove final classifications. Kruskal-Wallis tests showed significant differences in every channel attribute used in the geomorphic classification and Wilcoxon Rank Sum Tests identified pairwise differences ($p < 0.05$; Fig. 7). Because sediment size and valley confinement play an important role in clustering, the classification is broadly numerically organized from large to small clast size (Fig. 7). Channel types were also generally organized by confinement based on the median valley confinement value of each channel type (Fig. 7). While there was not a high log-log inverse correlation between sediment size and confinement using individual site data ($R^2 = 0.27$, $p < 0.01$), there is an inverse relationship between sediment size and valley confinement for median values of channel types 2 through 10 ($R^2 = 0.65$, $p < 0.01$). Figures depicting these relationships can be found in the Supplementary Information. Channel type 1 exists as a more unique setting within the basin and is discussed below.

Given the relationship between confinement and sediment size, the classification generally progresses from confined, mountainous upland streams with large sediment sizes to unconfined, lowland streams and rivers with small sediment. A notable exception is channel type 1, which fits within the conceptual framework of large to small sediment size rivers, but the sites exist in predominantly unconfined valleys. This lack of confinement indicates colluvial and mass movement processes are unlikely in these settings. Therefore, the large sediment clasts and unique Modoc Plateau volcanic terrain at these locations are either transported from upstream or non-fluvial legacy deposits of the underlying volcanic terrain (Hauer and Pulg, 2018).

6.2. Are *annual hydrological regimes* indicative of reach-scale morphology?

Statistical bootstrapping showed that the occurrences of hydrological settings within a given channel types were rarely statistically significant and thus the hydrological-geomorphic linkage was random (Fig. 8). To reiterate, significance is achieved when the actual number of sites in a hydrological setting for a given channel type or actual number of hydrological settings within a given channel type have a less than 5% probability of occurrence when compared to bootstrapping results. It should be noted that unlike the conceptual examples of bar plots given in graphics a1 and a2 of Figure 1, columns are not of the same height in Figure 8 due to unequal sampling of the channel types. However, the same tests can be applied. For the first test, the number of sites within a hydrological setting for each channel was found to be significant for three out of a possible 50 hydrological setting-channel type combinations (6% of all hydrological setting bins) ($p < 0.05$, Fig. 8a). All three significant findings are likely explained by the landscape features important in defining the annual hydrological regime. First, *boulder,*

667 *bed undulating* sites (n = 4) are unique along one river in HLP settings and likely due to
668 erosional processes producing a non-alluvial bed surface. Second, the abundance of
669 *high-gradient, step-pool/cascade* channels in LSR settings is attributed to the
670 dominance of LSR hydrologic patterns (e.g. snowmelt driven hydrology) in mountainous
671 regions of California where step-pool channels are also likely abundant. Third, 67% of
672 *low width-to-depth, gravel* sites exist within the RGW streams of the Central Valley of
673 California, which are characterized predominantly by relatively low slopes (<1%),
674 agricultural land use, and at times anastomosed streams.

675

676 While the previous three instances were significant, the second test showed that there
677 was little relation between number of hydrological settings and a channel type with only
678 two of ten channel types showing significance (20%) ($p < 0.05$; Fig. 8b). These
679 statistically significant returns are complementary to the first test and likely a product of
680 their landscape setting at the sub-basin scale rather than hydrology controlling the
681 channel type. Both statistical tests fell well below the proposed threshold of 70%
682 proposed to indicate clear hydrological control of channel types. Although 70% is
683 subjective, results of 6 and 20% are far below any reasonable definition of physical
684 control of one variable over another.

685

686 Hydrology was found to drive differences in gross dimensional channel attributes within
687 a channel type to a greater extent than feature attributes, but still below a majority level
688 of control. The greatest number of significant differences was found for the gross
689 dimensional attributes of w, w/d, and s ($p < 0.05$; Fig. 8c), however no attribute was

significant across more than 44% of channel types. Qualitative analysis of significant returns is as follows. Bankfull width was significantly higher in RGW settings ($p < 0.05$), which generally coincide with higher order streams lower in the basin. Therefore, bankfull width is likely to be larger based on downstream hydraulic geometry relationships. Confined, *gravel-cobble, uniform* streams are significantly smaller in HLP settings ($p < 0.05$), which is also consistent with increasing downstream hydraulic geometry because HLP settings have lower discharges compared with other annual hydrological regimes. However, significance in *w/d* does not show the same consistency as *w* as it both increases and decreases in tandem with hydrology in certain hydrological settings ($p < 0.05$). This precludes a simple explanation of the patterning of significance for bankfull width-to-depth ratio and may be due to landscape setting. Significant returns associated with slope may also be a result of landscape setting. Landscape influence can be observed as streams in three of nine channel types are significantly steeper in LSR settings ($p < 0.05$), which once again relates to the mountainous terrain in which this hydrologic setting is found.

6.3. Are *flood magnitudes* indicative of reach-scale morphology?

Statistical bootstrapping of flood magnitude settings showed more significant returns than annual hydrological regime, but still below a majority role. For the first bootstrapping test, 18.5% of tercile flood magnitude settings were significant (splits for low, medium, and high flood magnitude defined at 64 and 194 m^3/s) ($p < 0.05$; Fig. 9a). For the second test, which used decile flood magnitude settings (splits defined at 20.9, 34.9, 56.2, 92.8, 122.7, 152.1, 238.6, 373.9, and 592.7 m^3/s), the number of hydrological settings was significant for 40% of channel types ($p < 0.05$; Fig. 9b). Both results indicate that certain channel types exhibit basin scale flood magnitude-hydraulic geometry relationships, but similarities in reach-scale morphology appear predominantly governed by other factors. Therefore, flood magnitude does not appear to be a primary control on form between channel types but is rather only correlated to certain forms based upon where a specific channel type is found in the drainage network.

Rather than flood magnitude representing a difference between channel types, flood magnitude does explain differences in channel geometry within multiple channel types. Significant differences in gross geometry attributes exist across channel types (Fig. 9c). Bankfull width shows significant differences between flood magnitude settings in 67% of channel types ($p < 0.05$), which nearly exceeds the proposed significant threshold. Because flood magnitude was calculated from contributing area - discharge regressions, the significant differences associated with bankfull width are linked to well-established downstream hydraulic geometry relationships. Positive relationships between bankfull width and flood magnitude exist for several step-pool, uniform, and riffle-pool channel types as well as the channel type that likely includes anastomosed channels, although anastomosed channels were not specifically quantified, but qualitatively identified after classification (channel type 9). When combined, all basin sites demonstrate a clear relationship between bankfull width and flood magnitude (R^2 = 0.56, $p < 0.01$), and results also indicate that these downstream hydraulic geometry relationships hold true within individual channel types as well.

6.4. Are *dimensionless flood magnitudes* indicative of reach-scale morphology?

Statistical bootstrapping results suggest that dimensionless flood magnitude could not universally control channel type presence (Fig. 10). Under the first bootstrapping test, the number of hydrological setting occurrences were significant in 17% of tercile bins (splits for low, medium, and high dimensionless flood magnitude defined at 0.83 and 2.41) ($p < 0.05$; Fig. 10a; Table S5). For the second bootstrapping test, 30% of channel types displayed a significant number of 10-bin hydrological settings (splits defined at dimensionless flood magnitudes of 0.27, 0.48, 0.76, 1.06, 1.40, 1.83, 2.61, 4.56, and 9.40) ($p < 0.05$; Fig. 10b; Table S3). Both results are well below the suggested 70% threshold and are likely the result of spurious correlation between channel attributes and channel type. That is, streams with relatively small and large sediment sizes exhibit high and low dimensionless flood magnitude values, respectively. Therefore, dimensionless flood magnitude appears to be a poor indicator of reach-scale morphology overall.

While the majority of significant values were associated with feature attributes, dimensionless flood magnitude settings showed significant differences in slope, a gross dimensional attribute (Fig. 10c). In four channel types including cascade/step-pool (channel type 2), cobble uniform streams (channel types 5 and 7), and high w/d riffle-pool (channel type 8), slope was found to be significantly lower in sites with high dimensionless flood magnitudes. In the uniform streams, the lack of variability in channel depth and width and the expression of slope as a critical factor in reach-scale morphology is logical because equivalent transport capacities needed to transport equivalent sediment yields can be achieved with increased slope and decreased flow or decreased slope and increased flow (Lane, 1954). Other factors in channel types with more variability may dampen this slope relationship. The remaining significant attributes are dominated by feature attributes, predominantly D_{50} and D_{84}, which are likely attributable to spurious correlation rather than physical significance. Unlike channel width (Leopold and Maddock, 1953), sediment size is generally negatively correlated with contributing area or discharge for 2nd order and larger streams (Brummer and Montgomery, 2003; Knighton, 1980). This results in an inverse relationship between dimensionless flood magnitude, as calculated here, and sediment size, meaning that significant differences are likely to be accentuated in this analysis for D_{50} and D_{84}.

7. Discussion

7.1. Multivariate statistical channel classification

Multivariate statistical analysis was used here to generate a data-driven classification for the particular basin geomorphology (Kasprak et al., 2016; Sutfin et al., 2014), which is in contrast to classifications based on preconceived definitions of reach-scale morphology. This approach is preferable when there is uncertainty as to what channel types exist in a region, and the larger the region the more likely there will be such uncertainty. On the other hand, it is possible that the larger the region, there might exist rare, unique channel types missed by sampling and thus not represented in a data-driven classification methodology. Further difficulty in multivariate statistical classification arises when selecting the appropriate number of final channel types. The classification is likely to make more physical sense with fewer channel types due to large differences in just a few channel attributes, but it may not be representative of the true geomorphic variability in a region of interest. However, uncorrelated channel attributes not influential in the highest statistical splits will likely be uniform across types as more dissimilar sites are lumped together. Alternatively, retaining more channel types may capture more variability across more attributes, but the multivariate nature of clustering may be capturing differences that have no physical meaning or conflicting physical meaning on various branches of a hierarchical clustering dendrogram. Statistical tests that help in selecting the number of stream classes (e.g. the Hubert Index) were found to be more indicative of clustering based on valley confinement and sediment size, but less indicative of less statistically dominant differences in reach-scale morphology like TVAs, which are fundamental to hydraulic differences in forms and critical in many established channel classifications (e.g. plane bed vs. riffle-pool) (Montgomery and Buffington, 1997).

The reach-scale morphological classification for the Sacramento River basin expands upon a previously developed data-driven sub-classification by Lane et al. (2017b), which focused on sites in the LSR annual hydrological regime setting. In addition to an increased number of sites from four other annual hydrological regime settings, this classification quantified and accounted for valley confinement as opposed to using it only for qualitative interpretation in the previous classification. Five outcomes can be observed in a qualitative reconciliation between the two classifications: comparable channel types, sub-channel types exist in Lane et al. (2017b) compared to broader channel types in the present Sacramento basin classification, broader channel types exist in Lane et al. (2017b) compared to sub-channel types channel types in the present Sacramento basin classification, channel types in the present classification do not exist in Lane et al. (2017b), and channel types in Lane et al. (2017b) do not exist in present Sacramento basin classification. More detailed relationships between the two classifications are presented in Table 2.

The Sacramento River basin reach-scale classification generally corresponds with other established classification systems. Here, we place our statistically-derived classification in the context of two of the most influential reach-scale classifications: Montgomery and Buffington's classification of mountain systems (1997) and Rosgen's channel classification (1994, 1996). A large majority of stream classes defined by Montgomery and Buffington (1997) are represented here; however, a number of additional channel types and valley settings are represented in the Sacramento basin as well. It may be that in smaller and more homogeneous landscapes (e.g. all confined mountain streams) fewer channel types exist (Montgomery and Buffington, 1997). The Sacramento basin classification indicates that valley confinement setting is likely to be important in differentiating channel types and associated hydrogeomorphic processes in more heterogeneous landscapes. Overly simplistic or insufficient channel types may miss key differences in form that may be important to physical interpretation or ecohydraulic conditions. Rosgen's (1994, 1996) classification is more likely to encompass all channel types identified in the Sacramento Basin classification, but because it does not explicitly stratify channel types by valley confinement (which is not the same as Rosgen's entrenchment ratio), it misses an important landscape-scale topographic control on channel typology. Confinement plays an implicit role in the lettering in that system but is not alone at that level. Rosgen (1996) has an independent qualitative valley classification system. The Rosgen classification is broad in nature to span many channel types, but is not quantitatively tested and proven, so our proposed statistical methodology is likely superior within a specific basin by characterizing distinct and regionally appropriate reach-scale morphologies and their continuum within a specific river basin. Given the binned sampling approach used here, the presented channel types represent both commonly observed and rare reach-scale morphologies specific to the Sacramento basin, but likely unsuitable for other regions.

Classification methods should be applicable in any region and support development of channel types that are physically interpretable, correspond with other established channel classifications, and incorporate regionally specific information to tailor classifications to the particularities of the region that may not be captured in more narrowly defined or broad classifications (Montgomery and Buffington, 1997; Rosgen, 1996). This knowledge is key for fundamental understanding of regional river geomorphology and its interplay with hydrology. Furthermore, reach-scale classification may support efforts to conserve and restore aquatic and riparian ecosystems that are key challenges in modern water resources management. For instance, reach scale classifications can be used to refine flow - ecology relationships in well-established environmental flows methods such as ELOHA (Poff et al., 2010).

7.2. The relative influence of hydrological settings

Contrary to the common assumption and our hypothesis that certain channel types would occur only in select hydrological settings, the results presented here show that channel types almost always exist across all hydrological settings. The few channel types preferentially occurring in certain hydrological settings can be attributed to relationships between median geomorphic attributes and sub-basin scale hydrological conditions (e.g. hydraulic geometry). However, even for significant hydro-geomorphic relationships, hydrology does not preclude those channel types from also existing in other hydrological settings. Therefore, hydrological setting is unlikely to be the primary control on channel morphology or, if initially the primary control, it is consistently dampened throughout the channel network by other local processes that create each of various channel types. This indicates that reach-scale morphology must be a product of other geomorphic influences such as sediment regime, topography, or geology.

Channel hydraulics, a product of hydrology and topographic steering, play an important role in the formation of morphological units. Differences in hydraulics have been hypothesized as controls in the formation of various channel types, such as riffle-pool and step-pool channels (Church and Zimmermann, 2007; MacWilliams et al., 2006; Thompson, 1986; Zimmermann et al., 2010). In the case of channel hydraulics, sub-basin hydrology is more likely to change acutely at stream confluences, while topography can show abrupt, complex longitudinal change between tributary junctions, especially in mountainous terrain (Wohl, 2000). Variability among topographic variables can be independent or linked, yielding different functional landforms, and then these may be hierarchically nested at different flow stages to further complicate hydraulics to drive different morphological outcomes (Pasternack et al., 2018a, 2018b). This supports the idea that the existence of a given channel type is perhaps less informed by catchment hydrology and instead driven by topographic influences.

Sediment supply or non-fluvial bed material may also impact reach-scale morphology more directly than sub-basin hydrological conditions (Church, 2006; Friend, 1993; Harvey, 1991; Hauer and Pulg, 2018). Although substantial geomorphic change is often related to flood events, the sediment characteristics may control specific changes to channel form more than the amount of water (Wohl et al., 2015). For example, Tooth and Nanson (2004) demonstrate two arid region rivers with similar discharge regimes but different morphologies partially attributed to sediment caliber. In conjunction and at a continental scale, Phillips and Jerolmack (2016) concluded that channels self-organize shape to achieve a critical shear depth needed to transport available bed sediments during floods, which is exemplified by studies of bar and channel pattern dynamics associated with sediment fluxes in dammed and dam removal settings (East et al., 2015, 2018; Melis et al., 2012). Both examples point to reach-scale sediment conditions as important drivers of channel morphology. In regard to the channel classification presented here, confined streams are likely subjected to episodic but infrequent lateral inputs of sediment by mass movement events, while unconfined low gradient streams are likely subjected to more gradual, longitudinal sediment inputs (Benda and Dunne, 1997b, 1997a; Grant and Swanson, 1995). Finally, Sloan et al. (2001) noted that valley floor modification is less dependent on the magnitude and frequency of in-channel flood events and more dependent on the denudation of landscapes and mass movement events. Because results presented here show that annual hydrological regime, flood magnitude, and dimensionless flood magnitudes are not statistically related to the occurrence of channel types, it is possible that sediment supply in combination with size would be a better indicator of reach-scale morphology. Further, the known land-use changes across the Sacramento River basin and alterations in sediment regimes in a number of rivers may further drive dependence of channel types on sediment supply (Gilbert, 1917; James, 1991; White et al., 2010). Site specific sediment regimes were not the focus of this study but are an important avenue for future research.

Partial understanding of hydrological influence, or lack of influence, on reach-scale morphology can likely be accomplished through qualitative reasoning. For a specified stream location, observations of the reach-scale hydrology responsible for a given form are difficult to obtain except following a large channel-altering flood event (Dean and Schmidt, 2013). It may be possible to estimate bankfull channel discharge or flow depth necessary to entrain bed sediments, but when a flow has occurred and to what extent the channel shape was altered are not simple questions. Further complicating the relationships between form and hydrology, different channel types are likely formed and maintained under different flow magnitudes (Knighton, 1998). Similar forms are also found within different climatic conditions (e.g. temperate vs. arid) and thus subjected to large differences in annual hydrological conditions (Wohl and Merritt, 2008). In comparison, biological characteristics along a river reach are likely to display indicators related to recent flow patterns or events (e.g. riparian recruitment) and flows over longer periods of time (e.g. plant senescence) (Polvi et al., 2011). The fact that geomorphic characteristics are likely less relatable to recent flow events than through biological indicators may simply be representative of the low and high influences hydrology has on reach-scale geomorphic channel types and biological conditions, respectively. Individual morphological units can also be formed by local processes, for example in the formation of forced pool or riffle conditions involving bedrock or large woody debris (Fryirs and Brierley, 2012; Montgomery and Buffington, 1998). This clear evidence of morphological unit formation points toward local valley influences being key drivers of reach-scale morphology as opposed to sub-basin scale hydrological patterns as local geomorphic influences can dictate thresholds of geomorphic form (Montgomery, 1999; Poff et al., 2006).

7.3. Hydrological influence on topographic variability

Results from all hydrological analyses show relatively few significant differences in TVA values by hydrologic grouping. TVAs were identified as key attributes in distinguishing channel types, and different channel types exhibit differences in hydraulic patterns relevant to ecological functioning (Lane et al., 2018a). The hydrological metrics evaluated here do not capture significant differences in TVAs, and consequently do not control variability in channel dimensions. Montgomery (1999) conceptualized that continuum processes would likely be more influential on channel size, while channel morphology would be dependent on local controls. This study confirms that concept by showing that TVA values are not influenced by basin-scale hydrology. This is complementary to the fact that hydraulic geometry relationships exhibit variability around a median condition that cannot be ascribed to sub-basin hydrology (Park, 1977). If variability in form is not defined by basin-scale hydrology, then it is logical that reach-scale channel types, which are often defined by characteristic bedforms, are not related to hydrological conditions across a basin.

A number of extremal hypotheses have been suggested for the development of repeating channel patterns and forms and the majority fit within the context of the minimum energy principle (Huang et al., 2004). With depth variability shown here to be unrelated to hydrological settings and bedforms being a major component of energy dissipation in rivers (Davies and Sutherland, 1980), it would suggest that the nature of energy dissipation induced by stream form is primarily controlled by factors other than hydrology (e.g. lithology, topography, sediment supply, etc.). Langbein and Leopold (1964) note two distinct sources of variance in channels: that associated with variation around an average condition as a system searches for equilibrium and that which exists in any natural system because of local factors that make two systems inherently different. The latter form of variance at a sub-basin scale could conceptually be represented by distinct channel types. This would mean that channel types are far more

966 dependent on local valley topography and sediment supply. Hydrological events that
967 have been observed to cause large changes in channel widths and pattern (Yochum et
968 al., 2017), may be representative of variance around the average condition. This result
969 would suggest that channels take the reach-scale morphology of local conditions and
970 that reach-scale morphology is dimensionally adjusted to the continuum basin
971 conditions such as those defined by downstream hydraulic geometry relationships.
972
973 7.4. Hydrological analysis constraints
974
975 Although sub-basin hydrological settings provide limited information about the likelihood
976 of occurrence of a given channel type, study results do not preclude hydrological
977 influence on reach-scale morphology, such as through site-specific hydrology. Historical
978 flow conditions are likely to play a role in channel pattern at a minimum and when
979 thinking about at-a-station form at different flow magnitudes (Heitmuller et al., 2015).
980 Channel width expansion and contraction cycles have been linked to hydrological
981 disturbance events (Dean and Schmidt, 2013; Pizzuto, 1994; Sholtes et al., 2018) and
982 long-term effects of natural and anthropogenic alterations to river systems (Friedman et
983 al., 2015; Grams and Schmidt, 2002; Swanson et al., 2011). These documented
984 impacts of hydrological changes occur in channels where width expansion is possible
985 and are likely related to classic relationships of single and multi-threaded channels and
986 discharge (Leopold and Wolman, 1957; Schumm, 1977). Our final reach-scale
987 classification lacks a braided, gravel-bed river type which precludes the comparison
988 between single and multi-threaded river channels in this study. Even with a braided

channel type, at-a-station hydrological records are probably much more important to channel types than more commonly available extrapolated or modeled hydrological information.

Beyond historical flow events, consistent nuanced differences in at-a-station hydrology may also play a role in reach-scale morphology. Given that channel hydraulics create and maintain various morphological units and that hydraulics are a product of hydrology as well as topographic steering and biological influences, there may be differences in sub-basin hydrology at reach-scales associated with changing landscape conditions. Deal et al. (2018) note that climatic signals are often muted across basins due to landscape characteristics. Locations with less muted climatic signals and exhibiting median basin-scale hydrology may also display median hydraulic geometry tendencies. However, locations that do not display expected hydrology may lead to the scatter of channel types across hydrological groups demonstrated here. For example, in conjunction with distinct changes in slope and confinement, basin hydrology is observed to be highly altered on alluvial fans or in alpine meadows (Hooke, 1967; McClymont et al., 2010). A second possibility is that hydrological influences are most impactful at small catchment scales (Gomi et al., 2002). It is possible for two headwater basins to have distinctly different retention capacity and therefore also have different flood event magnitudes. Different inputs from two distinct basins will impact reach-scale morphology. For example, if a headwater basin is prone to debris flow conditions and is directly connected to a confined stream (Brummer and Montgomery, 2003; Rathburn et al., 2018), that basin will contribute considerably more sediment to the stream compared to a disconnected or low-sediment basin. If differences in debris flow susceptibility are driven by differences in hydrology, then hydrology is the key driver in that system. In addition, recovery times of channels subjected to disturbances would be dependent on hydrology as well (Wohl and Pearthree, 1991). Finally, reach-scale dynamics in sub-basin hydrology may also play a role in the vegetation communities along a channel reach, which can influence reach-scale morphology through processes such as bank or bar stabilization and channel narrowing (Gurnell, 2014). Therefore, hydrological importance does not necessarily need to be linked to the basin scale differences in hydrology that were examined here.

While results showed that sub-basin hydrology is a poor indicator of channel type, results may differ in basins with more unique hydrological settings. We may expect to find a number of cases where the findings presented here do not hold true, especially in peculiar places (Grant and O'Connor, 2003). While all rivers are unique, certain hydrological settings show more distinct characteristics. For example, rivers in karst environments have complex hydrodynamic and erosional characteristics that ultimately lead to substantial differences in hydrology and morphological form (Ford and Williams, 2007; Ritter et al., 1995). At these locations hydrogeomorphic correlations may be considerably more distinct. Other peculiar river environments likely exist that are observable at sub-basin hydrological scales, which would also contradict our findings.

Given that the Sacramento River basin has been subjected to a number of hydrogeomorphic alterations, as documented above, the basin itself could be one of the aforementioned peculiar places. It may be that the results presented here are not the norm and similar methodologies used in other portions of the world would show strong dependence of reach-scale channel types on the defining hydrology at a site. We view this as unlikely though for a few reasons. First, almost all rivers around the world have faced some anthropogenic impacts, so the idea of finding perfect locations to test the premise of this study is questionable. Second, in defense of the relevance of the Sacramento River basin for such testing, the results presented here conform with long standing hydrogeomorphic concepts of a link between form and process, such as predictable downstream hydraulic geometry. In the study basin, hydrology does display a noticeable relationship with bankfull width. How can one argue that the basin is too badly impacted to show real hydrological controls when it does in fact show a real discharge-based control on channel size? Therefore, the fact that reach-scale channel types do not appear to align with hydrological settings in this study would indicate that similar findings are likely to be found in other locations.

8. Conclusions

This study sought to address the following novel question: are sub-basin hydrological settings indicative of reach-scale morphology, or does reach-scale morphology exist independently of hydrological patterns within a basin? The statistically-derived channel types in the Sacramento River basin, a moderately sized catchment with high topographic and hydrological variability, were found to exist across almost all hydrological settings examined. Results from our statistical bootstrapping approach indicate that continuum hydrology is not a primary control on reach-scale morphologies, but instead only influences channel dimensions. Results further suggest that even median channel dimensions are often greatly altered by other geomorphic processes or controls. Given the hierarchical nature of rivers, this analysis only focuses on one scale of basin and channel morphology, so hydrology may still be an observable control at other scales. Isolation of potential reach-scale controls, such as hydrology, sediment supply, topography, and local geomorphic drivers, can infer the level of influence each has on reach-scale morphology through the rigorous statistical methodologies and should continue to be pursued for classification-based river management strategies.

References

Anderson MJ. 2001. A new method for non-parametric multivariate analysis of variance. Austral Ecology **26**: 32–46. DOI: 10.1111/j.1442-9993.2001.01070.pp.x

Bard A, Renard B, Lang M, Giuntoli I, Korck J, Koboltschnig G, Janža M, d'Amico M, Volken D. 2015. Trends in the hydrologic regime of Alpine rivers. Journal of Hydrology **529**: 1823–1837. DOI: 10.1016/j.jhydrol.2015.07.052

Beechie T, Buhle E, Ruckelshaus M, Fullerton A, Holsinger L. 2006. Hydrologic regime and the conservation of salmon life history diversity. Biological Conservation **130**: 560–572. DOI: 10.1016/j.biocon.2006.01.019

Beechie T, Imaki H. 2014. Predicting natural channel patterns based on landscape and geomorphic controls in the Columbia River basin, USA. Water Resources Research **50**: 39–57. DOI: 10.1002/2013WR013629

Benda L, Dunne T. 1997a. Stochastic forcing of sediment routing and storage in channel networks. Water Resources Research **33**: 2865–2880. DOI: 10.1029/97WR02387

Benda L, Dunne T. 1997b. Stochastic forcing of sediment supply to channel networks from landsliding and debris flow. Water Resources Research **33**: 2849–2863. DOI: 10.1029/97WR02388

Bisson PA, Montgomery DR, Buffington JM. 1996. Valley segments, stream reaches, and channel units. Methods in stream ecology : 23–52.

Brierley GJ, Fryirs K. 2000. River Styles, a Geomorphic Approach to Catchment Characterization: Implications for River Rehabilitation in Bega Catchment, New South Wales, Australia. Environmental Management **25**: 661–679. DOI: 10.1007/s002670010052

Brummer CJ, Montgomery DR. 2003. Downstream coarsening in headwater channels. Water Resources Research **39** DOI: 10.1029/2003WR001981 [online] Available from: https://agupubs.onlinelibrary.wiley.com/doi/abs/10.1029/2003WR001981 (Accessed 11 September 2018)

Buffington JM, Lisle TE, Woodsmith RD, Hilton S. 2002. Controls on the size and occurrence of pools in coarse-grained forest rivers. River Research and Applications **18**: 507–531. DOI: 10.1002/rra.693

Carson MA. 1972. Hillslope form and process. University Press: Cambridge

Carson MA. 1984. The meandering-braided river threshold: A reappraisal. Journal of Hydrology **73**: 315–334. DOI: 10.1016/0022-1694(84)90006-4

Chang HH. 1979. Minimum stream power and river channel patterns. Journal of Hydrology **41**: 303–327. DOI: 10.1016/0022-1694(79)90068-4

Chin A, Wohl EE. 2005. Toward a theory for step pools in stream channels. Progress in Physical Geography: Earth and Environment **29**: 275–296. DOI: 10.1191/0309133305pp449ra

Church M. 2002. Geomorphic thresholds in riverine landscapes. Freshwater biology **47**: 541–557.

Church M. 2006. Bed Material Transport and the Morphology of Alluvial River Channels. Annual Review of Earth and Planetary Sciences **34**: 325–354. DOI: 10.1146/annurev.earth.33.092203.122721

Church M, Zimmermann A. 2007. Form and stability of step-pool channels: Research progress. Water Resources Research **43** DOI: 10.1029/2006WR005037 [online] Available from: https://agupubs.onlinelibrary.wiley.com/doi/abs/10.1029/2006WR005037 (Accessed 27 August 2018)

Clarke KR. 1993. Non-parametric multivariate analyses of changes in community structure. Australian Journal of Ecology **18**: 117–143. DOI: 10.1111/j.1442-9993.1993.tb00438.x

Dahm CN, Grimm NB, Marmonier P, Valett HM, Vervier P. 1998. Nutrient dynamics at the interface between surface waters and groundwaters. Freshwater Biology **40**: 427–451. DOI: 10.1046/j.1365-2427.1998.00367.x

Davies TR, Sutherland AJ. 1980. Resistance to flow past deformable boundaries. Earth Surface Processes **5**: 175–179.

Davies TRH, Sutherland AJ. 1983. Extremal hypotheses for river behavior. Water Resources Research **19**: 141–148. DOI: 10.1029/WR019i001p00141

Deal E, Braun J, Botter G. 2018. Understanding the Role of Rainfall and Hydrology in Determining Fluvial Erosion Efficiency. Journal of Geophysical Research: Earth Surface **123**: 744–778. DOI: 10.1002/2017JF004393

Dean DJ, Schmidt JC. 2013. The geomorphic effectiveness of a large flood on the Rio Grande in the Big Bend region: Insights on geomorphic controls and post-flood geomorphic response. Geomorphology **201**: 183–198. DOI: 10.1016/j.geomorph.2013.06.020

De'ath G, Fabricius KE. 2000. Classification and Regression Trees: A Powerful yet Simple Technique for Ecological Data Analysis. Ecology **81**: 3178–3192. DOI: 10.1890/0012-9658(2000)081[3178:CARTAP]2.0.CO;2

East AE et al. 2015. Large-scale dam removal on the Elwha River, Washington, USA: River channel and floodplain geomorphic change. Geomorphology **228**: 765–786. DOI: 10.1016/j.geomorph.2014.08.028

East AE, Logan JB, Mastin MC, Ritchie AC, Bountry JA, Magirl CS, Sankey JB. 2018. Geomorphic Evolution of a Gravel-Bed River Under Sediment-Starved Versus Sediment-Rich Conditions: River Response to the World's Largest Dam Removal. Journal of Geophysical Research: Earth Surface **123**: 3338–3369. DOI: 10.1029/2018JF004703

ESRI. 2016. ArcGIS Desktop. Environmental Systems Research Institute: Redlands, CA

Filzmoser P, Garrett RG, Reimann C. 2005. Multivariate outlier detection in exploration geochemistry. Computers & Geosciences **31**: 579–587. DOI: 10.1016/j.cageo.2004.11.013

Filzmoser P, Gschwandtner M. 2012. mvoutlier: Multivariate outlier detection based on robust methods. R package version **1**

Flores AN, Bledsoe BP, Cuhaciyan CO, Wohl EE. 2006. Channel-reach morphology dependence on energy, scale, and hydroclimatic processes with implications for prediction using geospatial data. Water Resources Research **42** DOI: 10.1029/2005WR004226 [online] Available from: https://agupubs.onlinelibrary.wiley.com/doi/abs/10.1029/2005WR004226 (Accessed 12 September 2018)

Ford D, Williams PW. 2007. Karst hydrogeology and geomorphology . [Rev. ed.]. John Wiley & Sons: Chichester, England ; Hoboken, NJ

Friedman JM, Vincent KR, Griffin ER, Scott ML, Shafroth PB, Auble GT. 2015. Processes of arroyo filling in northern New Mexico, USA. Geological Society of America Bulletin **127**: 621–640.

Friend PF. 1993. Control of river morphology by the grain-size of sediment supplied. Sedimentary Geology **85**: 171–177. DOI: 10.1016/0037-0738(93)90081-F

Frissell CA, Liss WJ, Warren CE, Hurley MD. 1986. A hierarchical framework for stream habitat classification: Viewing streams in a watershed context. Environmental Management **10**: 199–214. DOI: 10.1007/BF01867358

Fryirs KA, Brierley GJ. 2012. Geomorphic Analysis of River Systems: An Approach to Reading the Landscape . John Wiley & Sons, Ltd: Chichester, UK [online] Available from: http://doi.wiley.com/10.1002/9781118305454 (Accessed 31 July 2018)

Fryirs KA, Wheaton JM, Brierley GJ. 2016. An approach for measuring confinement and assessing the influence of valley setting on river forms and processes. Earth Surface Processes and Landforms **41**: 701–710. DOI: 10.1002/esp.3893

Gesch D, Oimoen M, Greenlee S, Nelson C, Steuck M, Tyler D. 2002. The national elevation dataset. Photogrammetric engineering and remote sensing **68**: 5–32.

Gilbert GK. 1917. Hydraulic-mining debris in the Sierra Nevada . United States Geological Survey [online] Available from: https://doi.org/10.3133/pp105 (Accessed 26 September 2019)

Gilbert JT, Macfarlane WW, Wheaton JM. 2016. The Valley Bottom Extraction Tool (V-BET): A GIS tool for delineating valley bottoms across entire drainage networks. Computers & Geosciences **97**: 1–14. DOI: 10.1016/j.cageo.2016.07.014

Gomi T, Sidle RC, Richardson JS. 2002. Understanding Processes and Downstream Linkages of Headwater Systems. BioScience **52**: 905. DOI: 10.1641/0006-3568(2002)052[0905:UPADLO]2.0.CO;2

Graf WL. 1988. Fluvial processes in dryland rivers . Springer-Verlag: Berlin [online] Available from: https://scholar.google.com/scholar_lookup?title=Fluvial%20processes%20in%20dryland%20rivers&author=W.L.%20Graf&publication_year=1988 (Accessed 4 December 2018)

Grams PE, Schmidt JC. 2002. Streamflow regulation and multi-level flood plain formation: channel narrowing on the aggrading Green River in the eastern Uinta Mountains, Colorado and Utah. Geomorphology **44**: 337–360. DOI: 10.1016/S0169-555X(01)00182-9

Grant GE, O'Connor JE. 2003. A peculiar river: geology, geomorphology, and hydrology of the Deschutes River, Oregon . American Geophysical Union

Grant GE, Swanson FJ. 1995. Morphology and processes of valley floors in mountain streams, western Cascades, Oregon. Geophysical Monograph-American Geophysical Union **89**: 83–83.

Grant GE, Swanson FJ, Wolman MG. 1990. Pattern and origin of stepped-bed morphology in high-gradient streams, Western Cascades, Oregon. GSA Bulletin **102**: 340–352. DOI: 10.1130/0016-7606(1990)102<0340:PAOOSB>2.3.CO;2

Grill G et al. 2019. Mapping the world's free-flowing rivers. Nature **569**: 215–221. DOI: 10.1038/s41586-019-1111-9

Guinn JM. 1890. Exceptional years: a history of California floods and drought. Historical Society of Southern California, Los Angeles (1890) **1**: 33–39. DOI: 10.2307/41167825

Gurnell AM. 2014. Plants as river system engineers. Earth Surface Processes and Landforms **39**: 4–25. DOI: 10.1002/esp.3397

Gurnell AM et al. 2016. A multi-scale hierarchical framework for developing understanding of river behaviour to support river management. Aquatic Sciences **78**: 1–16. DOI: 10.1007/s00027-015-0424-5

Hack JT. 1960. Interpretation of erosional topography in humid temperate regions. American Journal of Science **258-A**: 80–97.

Harvey AM. 1991. The influence of sediment supply on the channel morphology of upland streams: Howgill Fells, Northwest England. Earth Surface Processes and Landforms **16**: 675–684. DOI: 10.1002/esp.3290160711

Hauer C, Pulg U. 2018. The non-fluvial nature of Western Norwegian rivers and the implications for channel patterns and sediment composition. CATENA **171**: 83–98. DOI: 10.1016/j.catena.2018.06.025

Heitmuller FT, Hudson PF, Asquith WH. 2015. Lithologic and hydrologic controls of mixed alluvial–bedrock channels in flood-prone fluvial systems: Bankfull and macrochannels in the Llano River watershed, central Texas, USA. Geomorphology **232**: 1–19. DOI: 10.1016/j.geomorph.2014.12.033

Hooke RLeB. 1967. Processes on Arid-Region Alluvial Fans. The Journal of Geology **75**: 438–460. DOI: 10.1086/627271

Huang HQ, Chang HH, Nanson GC. 2004. Minimum energy as the general form of critical flow and maximum flow efficiency and for explaining variations in river channel pattern. Water Resources Research **40** DOI: 10.1029/2003WR002539 [online] Available from: http://doi.wiley.com/10.1029/2003WR002539 (Accessed 26 February 2019)

James LA. 1991. Incision and morphologic evolution of an alluvial channel recovering from hydraulic mining sediment. Geological Society of America Bulletin **103**: 723–736.

Kabacoff RI. 2015. R in Action: Data analysis and graphis in R . 2nd ed. Manning Publications Co.: New York [online] Available from: https://www.manning.com/books/r-in-action-second-edition (Accessed 11 September 2019)

Kasprak A et al. 2016. The Blurred Line between Form and Process: A Comparison of Stream Channel Classification Frameworks. PLOS ONE **11**: e0150293. DOI: 10.1371/journal.pone.0150293

Knighton AD. 1980. Longitudinal changes in size and sorting of stream-bed material in four English rivers. GSA Bulletin **91**: 55–62. DOI: 10.1130/0016-7606(1980)91<55:LCISAS>2.0.CO;2

Knighton D. 1998. Fluvial Forms and Processes: A New Perspective . Routledge: New York, NY

Kondolf GM. 1997. Hungry Water: Effects of Dams and Gravel Mining on River Channels. Environmental Management **21**: 533–551. DOI: 10.1007/s002679900048

Kondolf GM, Piégay H, Schmitt L, Montgomery DR. 2016. Geomorphic classification of rivers and streams. In Tools in Fluvial Geomorphology , Kondolf GM and Piégay H (eds). John Wiley & Sons, Ltd; 133–158. [online] Available from: http://onlinelibrary.wiley.com/doi/10.1002/9781118648551.ch7/summary (Accessed 23 January 2018)

Kruskal JB. 1964. Multidimensional scaling by optimizing goodness of fit to a nonmetric hypothesis. Psychometrika **29**: 1–27. DOI: 10.1007/BF02289565

Lane BA, Dahlke HE, Pasternack GB, Sandoval-Solis S. 2017a. Revealing the Diversity of Natural Hydrologic Regimes in California with Relevance for Environmental Flows Applications. JAWRA Journal of the American Water Resources Association **53**: 411–430. DOI: 10.1111/1752-1688.12504

Lane BA, Pasternack GB, Dahlke HE, Sandoval-Solis S. 2017b. The role of topographic variability in river channel classification. Progress in Physical Geography : 0309133317718133. DOI: 10.1177/0309133317718133

Lane BA, Pasternack GB, Sandoval-Solis S. 2018a. Integrated analysis of flow, form, and function for river management and design testing. Ecohydrology DOI: 10.1002/eco.1969 [online] Available from: https://onlinelibrary.wiley.com/doi/abs/10.1002/eco.1969 (Accessed 9 April 2018)

Lane BA, Sandoval-Solis S, Stein ED, Yarnell SM, Pasternack GB, Dahlke HE. 2018b. Beyond Metrics? The Role of Hydrologic Baseline Archetypes in Environmental Water Management. Environmental Management DOI: 10.1007/s00267-018-1077-7 [online] Available from: http://link.springer.com/10.1007/s00267-018-1077-7 (Accessed 2 July 2018)

Lane EW. 1954. The importance of fluvial morphology in hydraulic engineering . Hyraulic Laboratory Report. U.S. Department of Interior - Bureau of Reclamation

Lane SN. 1995. The Dynamics of Dynamic River Channels. Geography **80**: 147–162.

Langbein WB, Leopold LB. 1964. Quasi-equilibrium states in channel morphology. American Journal of Science **262**: 782–794. DOI: 10.2475/ajs.262.6.782

Leopold LB, Maddock T. 1953. The Hydraulic Geometry of Stream Channels and Some Physiographic Implications

Leopold LB, Wolman MG. 1957. River channel patterns: Braided, meandering, and straight . USGS Numbered Series. U.S. Government Printing Office: Washington, D.C. [online] Available from: http://pubs.er.usgs.gov/publication/pp282B (Accessed 9 November 2018)

MacWilliams ML, Wheaton JM, Pasternack GB, Street RL, Kitanidis PK. 2006. Flow convergence routing hypothesis for pool-riffle maintenance in alluvial rivers. Water Resources Research **42**: W10427. DOI: 10.1029/2005WR004391

Makaske B. 2001. Anastomosing rivers: a review of their classification, origin and sedimentary products. Earth-Science Reviews **53**: 149–196. DOI: 10.1016/S0012-8252(00)00038-6

McClymont AF, Hayashi M, Bentley LR, Muir D, Ernst E. 2010. Groundwater flow and storage within an alpine meadow-talus complex. Hydrology and Earth System Sciences **14**: 859–872. DOI: 10.5194/hess-14-859-2010

McKay L, Bondelid T, Dewald T, Johnston J, Moore R, Rea A. 2012. NHDPlus version 2: user guide. US Environmental Protection Agency

Melis TS, Korman J, Kennedy TA. 2012. Abiotic & Biotic Responses of the Colorado River to Controlled Floods at Glen Canyon Dam, Arizona, Usa. River Research and Applications **28**: 764–776. DOI: 10.1002/rra.1503

Miller MC, McCAVE IN, Komar PD. 1977. Threshold of sediment motion under unidirectional currents. Sedimentology **24**: 507–527. DOI: 10.1111/j.1365-3091.1977.tb00136.x

Milliman JD, Syvitski JP. 1992. Geomorphic/tectonic control of sediment discharge to the ocean: the importance of small mountainous rivers. The Journal of Geology **100**: 525–544.

Moir HJ, Pasternack GB. 2010. Substrate requirements of spawning Chinook salmon (Oncorhynchus tshawytscha) are dependent on local channel hydraulics. River Research and Applications **26**: 456–468. DOI: 10.1002/rra.1292

Montgomery DR. 1999. Process Domains and the River Continuum. JAWRA Journal of the American Water Resources Association **35**: 397–410. DOI: 10.1111/j.1752-1688.1999.tb03598.x

Montgomery DR, Abbe TB, Buffington JM, Peterson NP, Schmidt KM, Stock JD. 1996. Distribution of bedrock and alluvial channels in forested mountain drainage basins. Nature **381**: 587–589. DOI: 10.1038/381587a0

Montgomery DR, Buffington JM. 1997. Channel-reach morphology in mountain drainage basins. Geological Society of America Bulletin **109**: 596–611.

Montgomery DR, Buffington JM. 1998. Channel processes, classification, and response. River Ecology and Management: Lessons from the Pacific Coastal Ecoregion, RJ Naiman and RE Bilby (Editors). Springer-Verlag, New York, New York : 13–42.

Mount JF. 1995. California rivers and streams: the conflict between fluvial process and land use . Univ of California Press

Murtagh F, Legendre P. 2014a. Ward's Hierarchical Agglomerative Clustering Method: Which Algorithms Implement Ward's Criterion? Journal of Classification **31**: 274–295. DOI: 10.1007/s00357-014-9161-z

Murtagh F, Legendre P. 2014b. Ward's Hierarchical Clustering Method: Clustering Criterion and Agglomerative Algorithm. Journal of Classification **31**: 274–295. DOI: 10.1007/s00357-014-9161-z

Neeson TM, Gorman AM, Whiting PJ, Koonce JF. 2008. Factors Affecting Accuracy of Stream Channel Slope Estimates Derived from Geographical Information Systems. North American Journal of Fisheries Management **28**: 722–732. DOI: 10.1577/M05-127.1

O'Brien GR, Wheaton JM, Fryirs K, Macfarlane WW, Brierley G, Whitehead K, Gilbert J, Volk C. 2019. Mapping Valley Bottom Confinement at the Network Scale. Earth Surface Processes and Landforms **0** DOI: 10.1002/esp.4615 [online] Available from: https://onlinelibrary.wiley.com/doi/abs/10.1002/esp.4615 (Accessed 28 March 2019)

Ode PR. 2007. Standard operating procedures for collecting benthic macroinvertebrate samples and associated physical and chemical data for ambient bioassessments in California. California State Water Resources Control Board. Surface Water Ambient Monitoring Program (SWAMP) Bioassessment SOP **1**

Oksanen J, Blanchet FG, Kindt R, Legendre P, Minchin PR, O'hara RB, Simpson GL, Solymos P, Stevens MHH, Wagner H. 2019. vegan: Community ecology package [online] Available from: https://CRAN.R-project.org/package=vegan

Omernik JM. 1987. Ecoregions of the Conterminous United States. Annals of the Association of American Geographers **77**: 118–125. DOI: 10.1111/j.1467-8306.1987.tb00149.x

Palmer T. 2012. Field guide to California rivers. Univ of California Press

Park CC. 1977. World-wide variations in hydraulic geometry exponents of stream channels: An analysis and some observations. Journal of Hydrology **33**: 133–146. DOI: 10.1016/0022-1694(77)90103-2

Parker G. 1979. Hydraulic geometry of active gravel rivers. Journal of the Hydraulics Division **105**: 1185–1201.

Parrett C, Veilleux A, Stedinger JR, Barth NA, Knifong DL, Ferris JC. 2011. Regional skew for California, and flood frequency for selected sites in the Sacramento-San Joaquin River Basin, based on data through water year 2006 . U. S. Geological Survey

Pasternack GB, Baig D, Weber MD, Brown RA. 2018a. Hierarchically nested river landform sequences. Part 1: Theory. Earth Surface Processes and Landforms **43**: 2510–2518. DOI: 10.1002/esp.4411

Pasternack GB, Baig D, Weber MD, Brown RA. 2018b. Hierarchically nested river landform sequences. Part 2: Bankfull channel morphodynamics governed by valley nesting structure. Earth Surface Processes and Landforms **43**: 2519–2532. DOI: 10.1002/esp.4410

Pfeiffer AM, Finnegan NJ, Willenbring JK. 2017. Sediment supply controls equilibrium channel geometry in gravel rivers. Proceedings of the National Academy of Sciences **114**: 3346–3351. DOI: 10.1073/pnas.1612907114

Phillips CB, Jerolmack DJ. 2016. Self-organization of river channels as a critical filter on climate signals. Science **352**: 694–697. DOI: 10.1126/science.aad3348

Pitlick J, Cress R. 2002. Downstream changes in the channel geometry of a large gravel bed river. Water Resources Research **38**: 34-1-34–11. DOI: 10.1029/2001WR000898

Pizzuto JE. 1994. Channel adjustments to changing discharges, Powder River, Montana. Geological Society of America Bulletin **106**: 1494–1501. DOI: 10.1130/0016-7606(1994)106<1494:CATCDP>2.3.CO;2

Poff NL et al. 2010. The ecological limits of hydrologic alteration (ELOHA): a new framework for developing regional environmental flow standards. Freshwater Biology **55**: 147–170.

Poff NL, Allan JD, Bain MB, Karr JR, Prestegaard KL, Richter BD, Sparks RE, Stromberg JC. 1997. The natural flow regime. BioScience: 769–784.

Poff NL, Bledsoe BP, Cuhaciyan CO. 2006. Hydrologic variation with land use across the contiguous United States: Geomorphic and ecological consequences for stream ecosystems. Geomorphology **79**: 264–285. DOI: 10.1016/j.geomorph.2006.06.032

Polvi LE, Wohl EE, Merritt DM. 2011. Geomorphic and process domain controls on riparian zones in the Colorado Front Range. Geomorphology **125**: 504–516. DOI: 10.1016/j.geomorph.2010.10.012

PRISM Climate Group. 2007. Oregon State University [online] Available from: http://prism.oregonstate.edu

R Core Team. 2017. R: A Language and Environment for Statistical Computing. R Foundation for Statistical Computing: Vienna, Austria [online] Available from: https://www.R-project.org/

Rathburn SL, Shahverdian SM, Ryan SE. 2018. Post-disturbance sediment recovery: Implications for watershed resilience. Geomorphology **305**: 61–75. DOI: 10.1016/j.geomorph.2017.08.039

Reid I, Laronne JB. 1995. Bed Load Sediment Transport in an Ephemeral Stream and a Comparison with Seasonal and Perennial Counterparts. Water Resources Research **31**: 773–781. DOI: 10.1029/94WR02233

Richards KS. 1977. Channel and flow geometry: a geomorphological perspective. Progress in Physical Geography: Earth and Environment **1**: 65–102. DOI: 10.1177/030913337700100105

Ritter DF, Kochel RC, Miller JR, Miller JR. 1995. Process geomorphology. Wm. C. Brown Dubuque, IA

Rosgen DL. 1994. A classification of natural rivers. CATENA **22**: 169–199. DOI: 10.1016/0341-8162(94)90001-9

Rosgen DL. 1996. Applied river morphology. Wildland Hydrology

Schumm SA. 1977. The fluvial system. Wiley: New York

Shields A. 1936. Application of similarity principles and turbulence research to bed-load movement

Sholtes JS, Yochum SE, Scott JA, Bledsoe BP. 2018. Longitudinal variability of geomorphic response to floods: Geomorphic response to floods. Earth Surface Processes and Landforms DOI: 10.1002/esp.4472 [online] Available from: http://doi.wiley.com/10.1002/esp.4472 (Accessed 24 September 2018)

Singer MB. 2007. The influence of major dams on hydrology through the drainage network of the Sacramento River basin, California. River Research and Applications **23**: 55–72. DOI: 10.1002/rra.968

Sloan J, Miller JR, Lancaster N. 2001. Response and recovery of the Eel River, California, and its tributaries to floods in 1955, 1964, and 1997. Geomorphology **36**: 129–154. DOI: 10.1016/S0169-555X(00)00037-4

Snow RS. 1989. Fractal sinuosity of stream channels. Pure and applied geophysics **131**: 99–109.

Sutfin NA, Shaw JR, Wohl EE, Cooper DJ. 2014. A geomorphic classification of ephemeral channels in a mountainous, arid region, southwestern Arizona, USA. Geomorphology **221**: 164–175. DOI: 10.1016/j.geomorph.2014.06.005

Swanson BJ, Meyer GA, Coonrod JE. 2011. Historical channel narrowing along the Rio Grande near Albuquerque, New Mexico in response to peak discharge reductions and engineering: magnitude and uncertainty of change from air photo measurements. Earth Surface Processes and Landforms **36**: 885–900. DOI: 10.1002/esp.2119

Thanapakpawin P, Richey J, Thomas D, Rodda S, Campbell B, Logsdon M. 2007. Effects of landuse change on the hydrologic regime of the Mae Chaem river basin, NW Thailand. Journal of Hydrology **334**: 215–230. DOI: 10.1016/j.jhydrol.2006.10.012

Therneau TM, Atkinson EJ. 2018. rpart: Recursive Partitioning and Regression Trees. . Mayo Foundation [online] Available from: https://CRAN.R-project.org/package=rpart

Thompson A. 1986. Secondary flows and the pool-riffle unit: A case study of the processes of meander development. Earth Surface Processes and Landforms **11**: 631–641. DOI: 10.1002/esp.3290110606

Tooth S. 2000. Process, form and change in dryland rivers: a review of recent research. Earth-Science Reviews **51**: 67–107. DOI: 10.1016/S0012-8252(00)00014-3

Tooth S, Nanson GC. 2004. Forms and processes of two highly contrasting rivers in arid central Australia, and the implications for channel-pattern discrimination and prediction. GSA Bulletin **116**: 802–816. DOI: 10.1130/B25308.1

USGS. 2016. GAP/LANDFIRE National Terrestrial Ecosystems 2011. DOI: 10.5066/f7zs2tm0 [online] Available from: https://www.sciencebase.gov/catalog/item/573cc51be4b0dae0d5e4b0c5 (Accessed 30 September 2019)

Ward JHJ. 1963. Hierarchical Grouping to Optimize an Objective Function. Journal of the American Statistical Association **58**: 236–244. DOI: 10.1080/01621459.1963.10500845

White JQ, Pasternack GB, Moir HJ. 2010. Valley width variation influences riffle–pool location and persistence on a rapidly incising gravel-bed river. Geomorphology **121**: 206–221. DOI: 10.1016/j.geomorph.2010.04.012

Wohl E, Bledsoe BP, Jacobson RB, Poff NL, Rathburn SL, Walters DM, Wilcox AC. 2015. The Natural Sediment Regime in Rivers: Broadening the Foundation for Ecosystem Management. BioScience **65**: 358–371. DOI: 10.1093/biosci/biv002

Wohl EE. 2000. Mountain rivers

Wohl EE. 2010. A brief review of the process domain concept and its application to quantifying sediment dynamics in bedrock canyons. Terra Nova **22**: 411–416. DOI: 10.1111/j.1365-3121.2010.00950.x

Wohl EE. 2013. The complexity of the real world in the context of the field tradition in geomorphology. Geomorphology **200**: 50–58. DOI: 10.1016/j.geomorph.2012.12.016

Wohl EE, Merritt DM. 2008. Reach-scale channel geometry of mountain streams. Geomorphology **93**: 168–185. DOI: 10.1016/j.geomorph.2007.02.014

Wohl EE, Pearthree PP. 1991. Debris flows as geomorphic agents in the Huachuca Mountains of southeastern Arizona. Geomorphology **4**: 273–292. DOI: 10.1016/0169-555X(91)90010-8

Wolman MG. 1954. A method of sampling coarse river-bed material. Eos, Transactions American Geophysical Union **35**: 951–956. DOI: 10.1029/TR035i006p00951

Wyrick JR, Pasternack GB. 2014. Geospatial organization of fluvial landforms in a gravel–cobble river: Beyond the riffle–pool couplet. Geomorphology **213**: 48–65. DOI: 10.1016/j.geomorph.2013.12.040

Yang CT, Song CCS, Woldenberg MJ. 1981. Hydraulic geometry and minimum rate of energy dissipation. Water Resources Research **17**: 1014–1018. DOI: 10.1029/WR017i004p01014

Yang D, Kane DL, Hinzman LD, Zhang X, Zhang T, Ye H. 2002. Siberian Lena River hydrologic regime and recent change. Journal of Geophysical Research: Atmospheres **107**: ACL 14-1-ACL 14-10. DOI: 10.1029/2002JD002542

Yochum SE, Sholtes JS, Scott JA, Bledsoe BP. 2017. Stream power framework for predicting geomorphic change: The 2013 Colorado Front Range flood. Geomorphology **292**: 178–192.

Zimmermann A, Church M, Hassan MA. 2010. Step-pool stability: Testing the jammed state hypothesis. Journal of Geophysical Research: Earth Surface **115** DOI: 10.1029/2009JF001365 [online] Available from: http://doi.wiley.com/10.1029/2009JF001365 (Accessed 27 August 2018)

Acknowledgements

This research was supported by the California State Water Resources Control Board under grant number 16-062-300. We also acknowledge the USDA National Institute of Food and Agriculture, Hatch project numbers #CA-D-LAW-7034-H and CA-D-LAW-2243-H. Finally, we would like to thank Brianna Ordung and John Deane for their roles in field data collection.

Figure 1. Conceptual diagram representing the experimental design used in this study. In the results box, graphics (a1) and (b1) illustrate the possible outcome in which hydrological setting has no explanatory power to differentiate among any channel types or any channel attributes. In graphics (a2) and (b2), hydrological setting is envisioned to have predominant explanatory power over channel types.

Figure 2. Map of the Sacramento River basin showing 288 stream survey locations among 2nd order and larger streams.

Figure 3. Hydrological settings binned by stream length for (a) annual hydrological regime (derived from Lane et al, 2018b) and (b) flood magnitude (adapted from Parrett et al. 2011), and by site for (c) dimensionless flood magnitude.

Figure 4. A conceptual example of how individual Kruskal-Wallis tests between hydrological settings are represented in a compact binary plot for each attribute in each channel type. Box-and-whisker plots are shown for channel type 4 only. A grey box in the binary plot represents a significant difference between hydrological settings for a given attribute ($p < 0.05$), while a white box represents an absence of a significant difference.

Figure 5. Results from a) non-metric multidimensional scaling and principal component analysis, b) hierarchical clustering by Ward's algorithm analyses, and c) classification tree. Vector length in (a) represents the influence on the clustering in the first two

dimensions (A_c is contributing area, *s* is surveyed slope, *d* is bankfull depth, *w* is bankfull width, *w/d* is bankfull width-to-depth ratio, CV_d is coefficient of variation in bankfull depth, CV_w is coefficient of variation in bankfull width, D_{84} is sediment size at the 84th percentile, and C_v is valley confinement; dashed lines only an aid to indicate which attribute is associated with which vector).

Figure 6. The ten channel types for the Sacramento River basin determined by multivariate statistical analysis with heuristic refinement.

Figure 7. Box and whisker plots representing differences in geomorphic attributes between channel types. Purple boxes represent channel types significantly different than multiple other channel types, orange boxes represent channel types significantly different than one other channel type, and white boxes represent no significant differences from all other channel types ($p < 0.05$). (A_c is contributing area, *s* is surveyed slope, *d* is bankfull depth, *w* is bankfull width, *w/d* is bankfull width-to-depth ratio, CV_d is coefficient of variation in bankfull depth, CV_w is coefficient of variation in bankfull width, D_{84} is sediment size at the 84th percentile, and C_v is valley confinement.)

Figure 8. Statistical analysis of reach-scale morphology – annual hydrological regime relationships including (a) and (b) the proportion of each channel type falling within each annual hydrological regime bin, and (c) a binary display of channel attribute significance between annual hydrological regime bins within a channel type. In the bar plots, black borders indicate that (a) the number of channel type sites within a hydrological setting or (b) the number of hydrological settings within a channel type have a less than 5%

probability of occurrence when compared to bootstrapping results. In (c), a grey rectangle represents a significant difference ($p < 0.05$).

Figure 9. Statistical analysis of reach-scale morphology – flood magnitude relationships including (a) the proportion of each channel type falling within tercile bins, (b) the proportion of each channel type falling within ten quantile bins labeled by the upper value of flood magnitude, and (c) a binary display of channel attribute significance between flood magnitude bins within a channel type. In the bar plots, black borders indicate that (a) the number of channel type sites within a hydrological setting or (b) the number of hydrological settings within a channel type have a less than 5% probability of occurrence when compared to bootstrapping results. In (c), a grey rectangle represents a significant difference ($p < 0.05$).

Figure 10. Statistical analysis of reach-scale morphology – dimensionless flood magnitude relationships including (a) the proportion of each channel type falling within tercile bins, (b) the proportion of each channel type falling within ten quantile bins labeled by the upper value of dimensionless flood magnitude, and (c) a binary display of channel attribute significance between dimensionless flood magnitude bins within a channel type. In the bar plots, black borders indicate that (a) the number of channel type sites within a hydrological setting or (b) the number of hydrological settings within a channel type have a less than 5% probability of occurrence when compared to bootstrapping results. In (c), a grey rectangle represents a significant difference ($p < 0.05$).

Table 1. Description of annual hydrological regimes within the Sacramento River Basin (Adapted from Lane et al. (2017a, 2018b))

Class	Hydrological Classification	Hydrological Characteristics	Physical and Climatic Catchment Controls
HLP (25 sites)	High elevation, low precipitation	• Upland streams with low discharge, but a distinct snowmelt pulse	• Catchments predominantly located on the Modoc Plateau • High elevations and dominated by volcanic rock and high organic content soils
LSR (120 sites)	Low-volume snowmelt and rain	• Transition between snowmelt and high-volume snowmelt and rain • Bimodal with distinct spring snowmelt pulse and winter rain peaks	• Mid-elevation catchments with limited contributing areas and low winter temperatures
PGR (54 sites)	Perennial groundwater and rain	• Characteristics of winter storms (predictable winter rain events) and groundwater (low seasonality), but generally stable flows	• Low elevation catchments with low riparian soils clay content or underlain by residual sedimentary rock materials
RGW (51 sites)	Rain and seasonal groundwater	• Bimodal hydrograph driven by predictable winter rains and supplemented at other times by groundwater	• Low elevation catchments with limited winter precipitation often associated with igneous and metamorphic rock materials • Coastal catchments with small aquifers driving short residence times
WS (38 sites)	Winter storms	• Predictable large fall and winter rainfall with January peak flows	• Low elevation catchments with substantial winter precipitation

Table 2. Reconciliation of the morphological classification presented here with that presented in Lane et al. (2017b).

Reconciliation Outcomes	**Lane et al. (2017b) channel types**	**Sacramento Basin channel types**	**Cause of reconciliation outcome**
1. Comparable channel types	• Confined headwater small boulder-cascade • Partly-confined large uniform • Unconfined large uniform boulder	• Confined boulder high-gradient step-pool/cascade • Partly-confined cobble-boulder uniform • Unconfined boulder-bedrock bed undulating	• Channel types that exist across both classifications are likely defined by distinct channel attributes and exist across a wide variety of landscapes • Differences in channel type naming strategies and final statistics that drive nomenclature result in different channel type names
2. Sub-classifications in Lane et al. (2017b) compared to broader channel types in present Sacramento basin classification	• Unconfined upland plateau large uniform • Unconfined anastomosing plateau small pool-riffle • Partly-confined expansion pool-wide bar	• Unconfined low w/d gravel • Partly-confined high w/d gravel-cobble riffle-pool	• When combined with a larger number of sites across various landscape settings, unconfined plateau and partly-confined expansion sites do not statistically differentiate themselves from other unconfined and partly-confined sites, respectively
3. Broader classifications in Lane et al. (2017b) represented by multiple channel types in present Sacramento basin classification	• Partly-confined pool-riffle • Confined cascade/step-pool	• Partly-confined high w/d gravel-cobble riffle-pool • Partly-confined low w/d gravel-cobble riffle-pool • Confined boulder-bedrock low-gradient step-pool • Confined boulder-bedrock uniform	• Differences in *w/d* proved significant to define two types of riffle-pool streams in partly-confined settings, while variability metrics differentiated between step-pool and uniform streams of similar slope
4. Channel types in the present classification do not exist in Lane et al. (2017b)	______	• Confined gravel-cobble uniform • Unconfined gravel-cobble riffle-pool	• Channel types exist in current classification, but not in Lane et al. (2017b) due to the addition of sites in other landscape settings
5. Channel types in Lane et al. (2017b) do not exist in present Sacramento basin classification	• Unconfined large meandering sand bed	______	• Changes in the defining hydrological settings of certain sites was changed between morphological classifications leading to those sites being excluded from the present classification (Lane et al., 2018b).

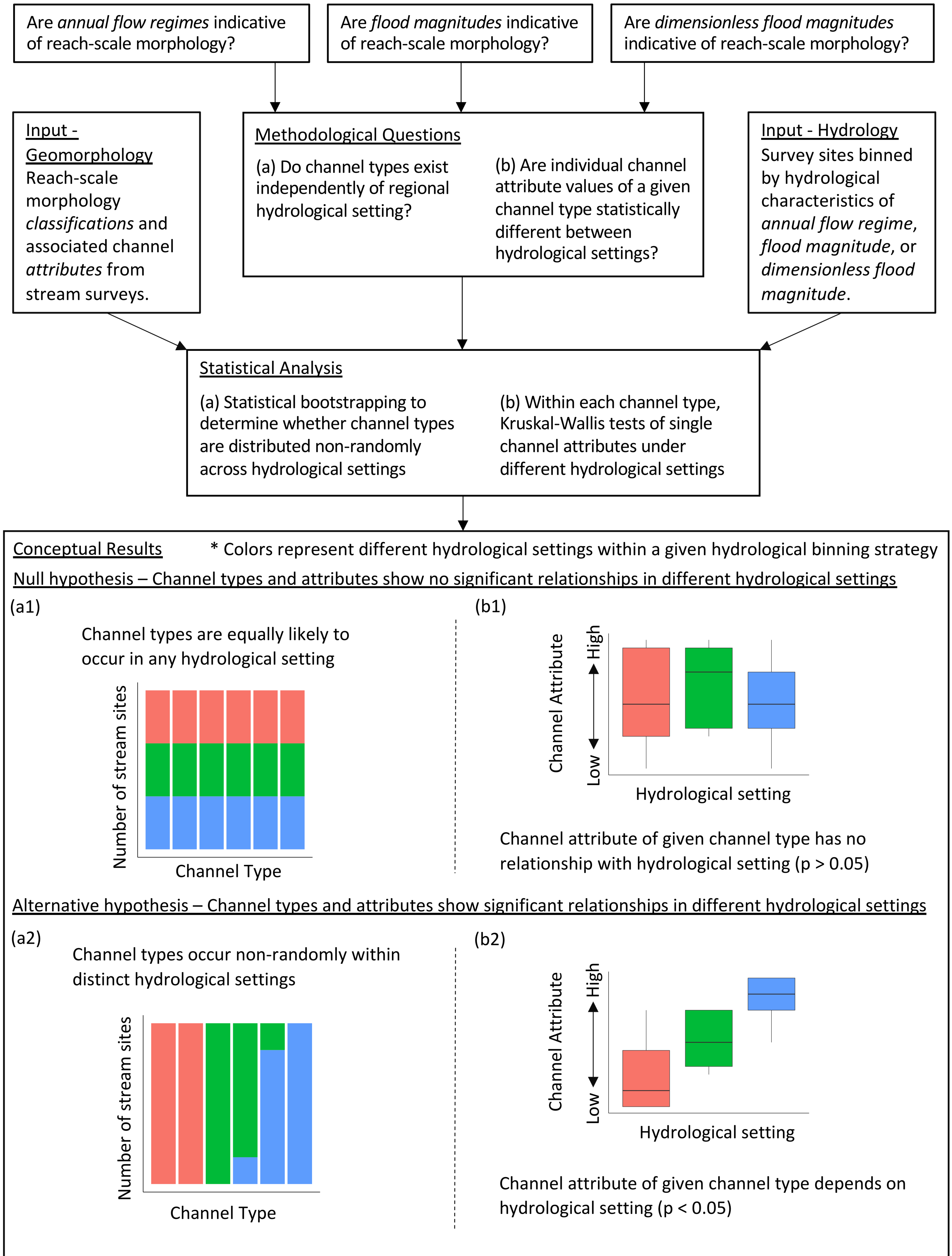
Are *annual flow regimes* indicative of reach-scale morphology?
Are *flood magnitudes* indicative of reach-scale morphology?
Are *dimensionless flood magnitudes* indicative of reach-scale morphology?
Input - Geomorphology
Reach-scale morphology *classifications* and associated channel *attributes* from stream surveys.
Methodological Questions
(a) Do channel types exist independently of regional hydrological setting?
(b) Are individual channel attribute values of a given channel type statistically different between hydrological settings?
Input - Hydrology
Survey sites binned by hydrological characteristics of *annual flow regime*, *flood magnitude*, or *dimensionless flood magnitude*.
Statistical Analysis
(a) Statistical bootstrapping to determine whether channel types are distributed non-randomly across hydrological settings
(b) Within each channel type, Kruskal-Wallis tests of single channel attributes under different hydrological settings
Conceptual Results
* Colors represent different hydrological settings within a given hydrological binning strategy
Null hypothesis – Channel types and attributes show no significant relationships in different hydrological settings
(a1)
Channel types are equally likely to occur in any hydrological setting
Number of stream sites
Channel Type
(b1)
Channel Attribute
High
Low
Hydrological setting
Channel attribute of given channel type has no relationship with hydrological setting (p > 0.05)
Alternative hypothesis – Channel types and attributes show significant relationships in different hydrological settings
(a2)
Channel types occur non-randomly within distinct hydrological settings
Number of stream sites
Channel Type
(b2)
Channel Attribute
High
Low
Hydrological setting
Channel attribute of given channel type depends on hydrological setting (p < 0.05)

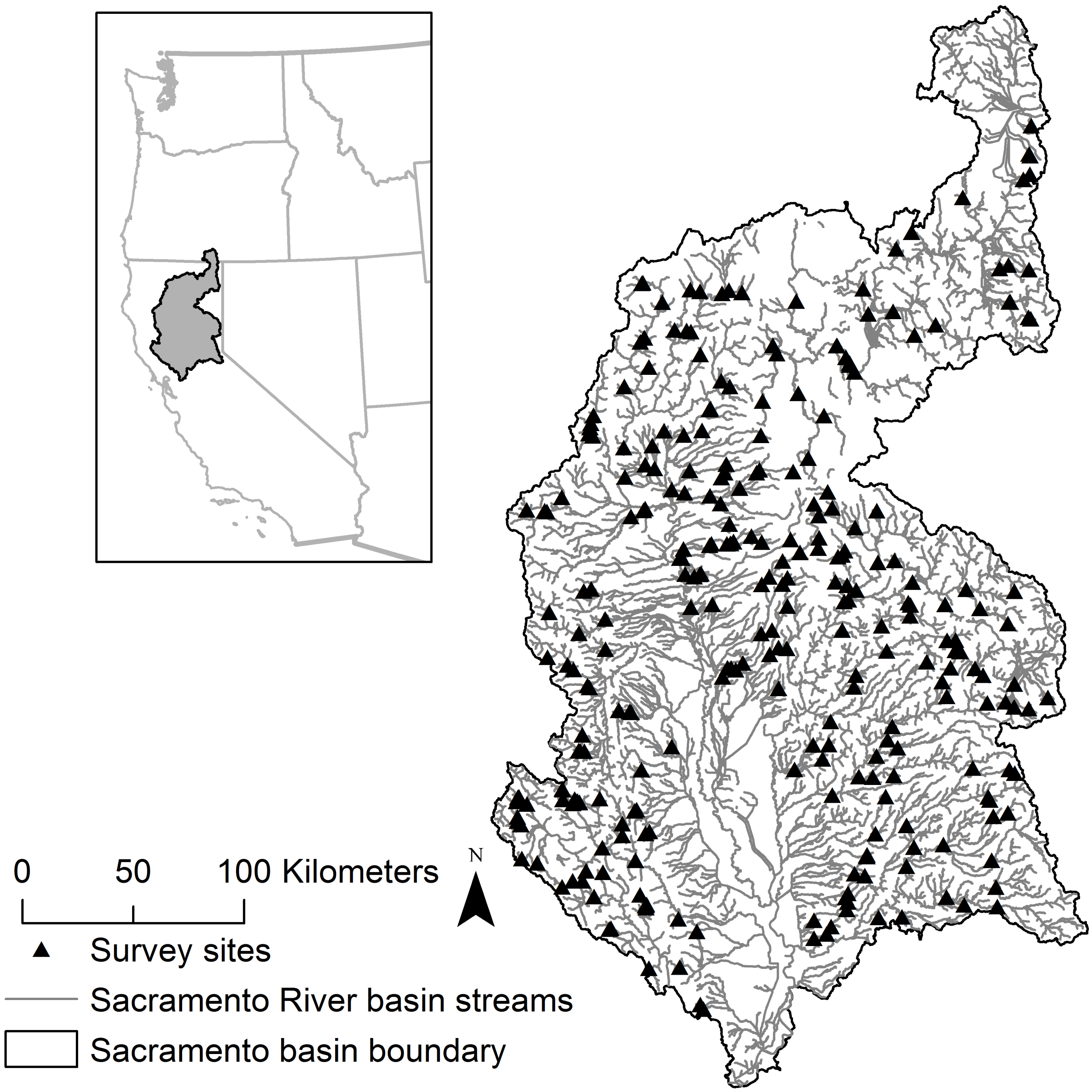
0 50 100 Kilometers
N
Survey sites
Sacramento River basin streams
Sacramento basin boundary

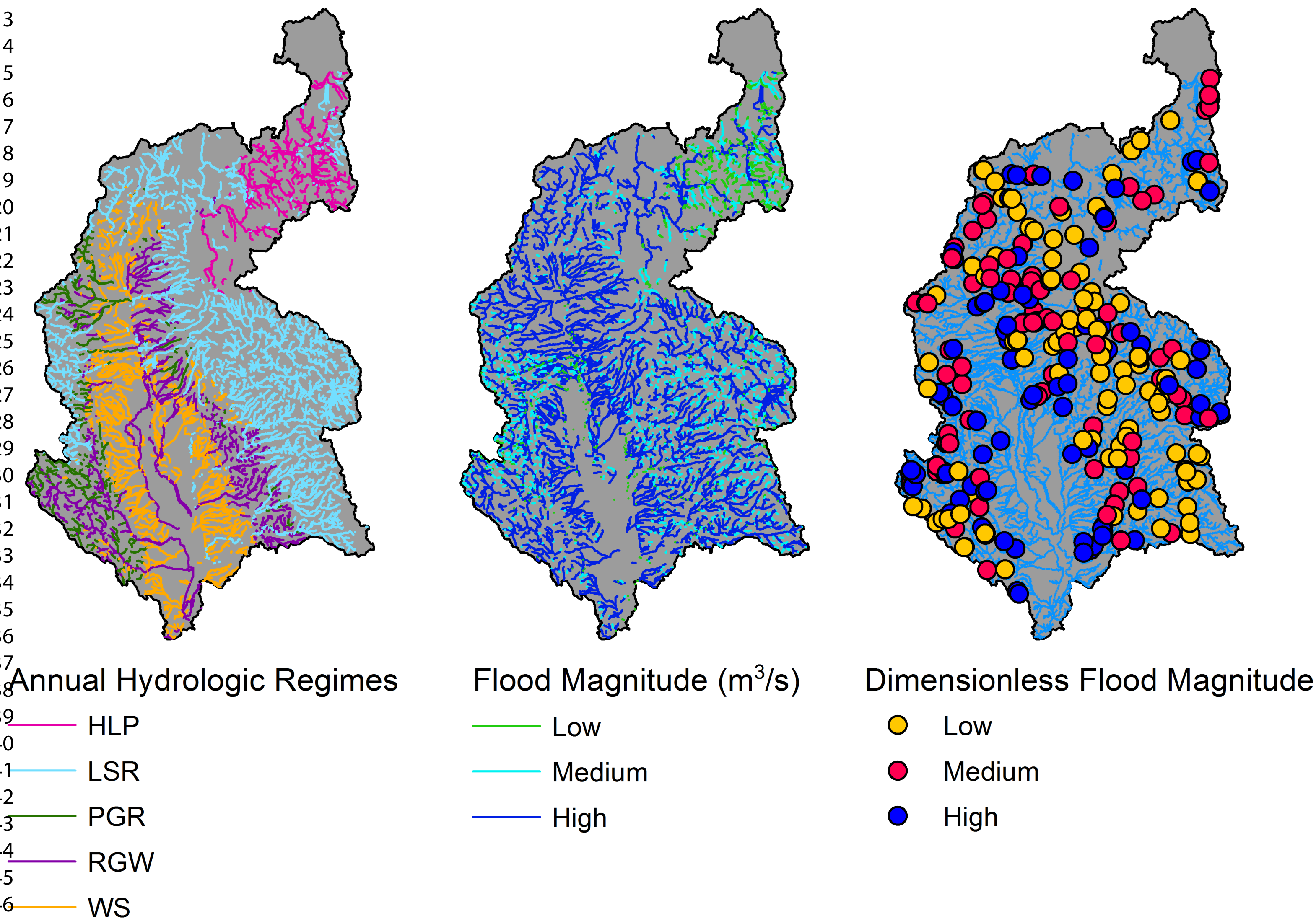
Annual Hydrologic Regimes
HLP
LSR
PGR
RGW
WS
Flood Magnitude (m³/s)
Low
Medium
High
Dimensionless Flood Magnitude
Low
Medium
High

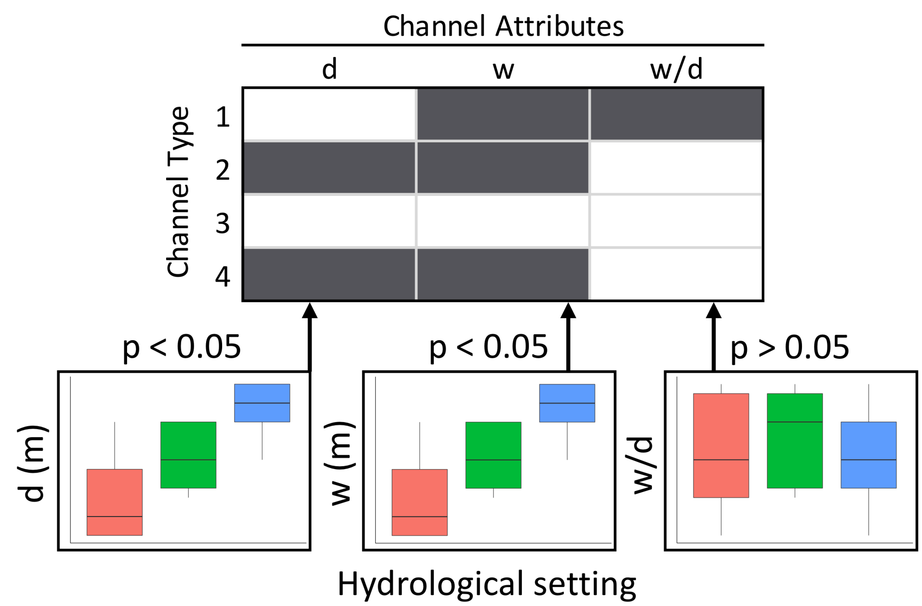
Channel Attributes
d
w
w/d
Channel Type
1
2
3
4
p < 0.05
p < 0.05
p > 0.05
d (m)
w (m)
w/d
Hydrological setting

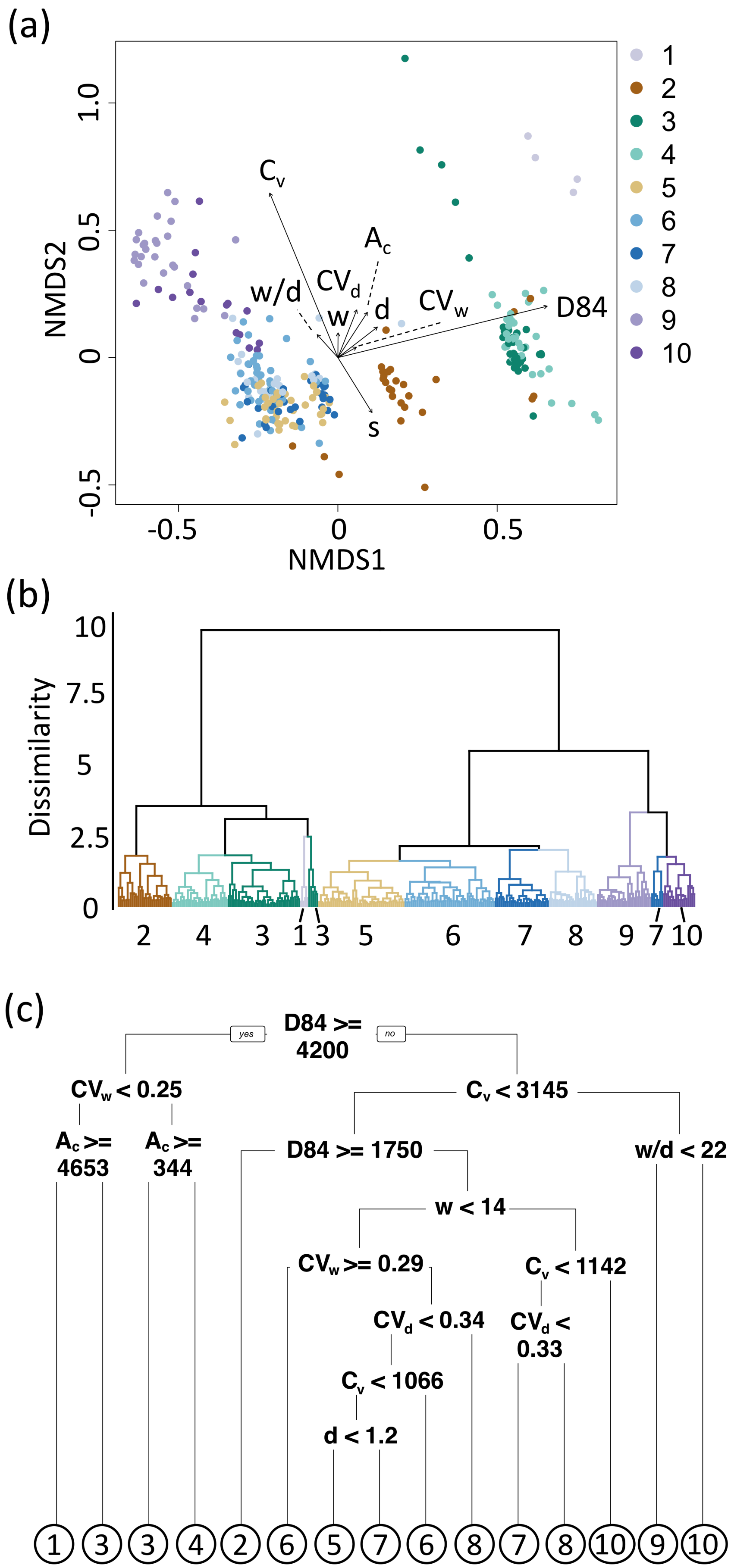
(a)
NMDS2
NMDS1
1.0
0.5
0
-0.5
-0.5
0
0.5
C_v
A_c
CV_d
w/d
w
d
CV_w
D84
s
1
2
3
4
5
6
7
8
9
10
(b)
Dissimilarity
10
7.5
5
2.5
0
2 4 3 1 3 5 6 7 8 9 7 10
(c)
yes
D84 >= 4200
no
CV_w < 0.25
C_v < 3145
A_c >= 4653
A_c >= 344
D84 >= 1750
w/d < 22
w < 14
CV_w >= 0.29
C_v < 1142
CV_d < 0.34
CV_d < 0.33
C_v < 1066
d < 1.2
1 3 3 4 2 6 5 7 6 8 7 8 10 9 10

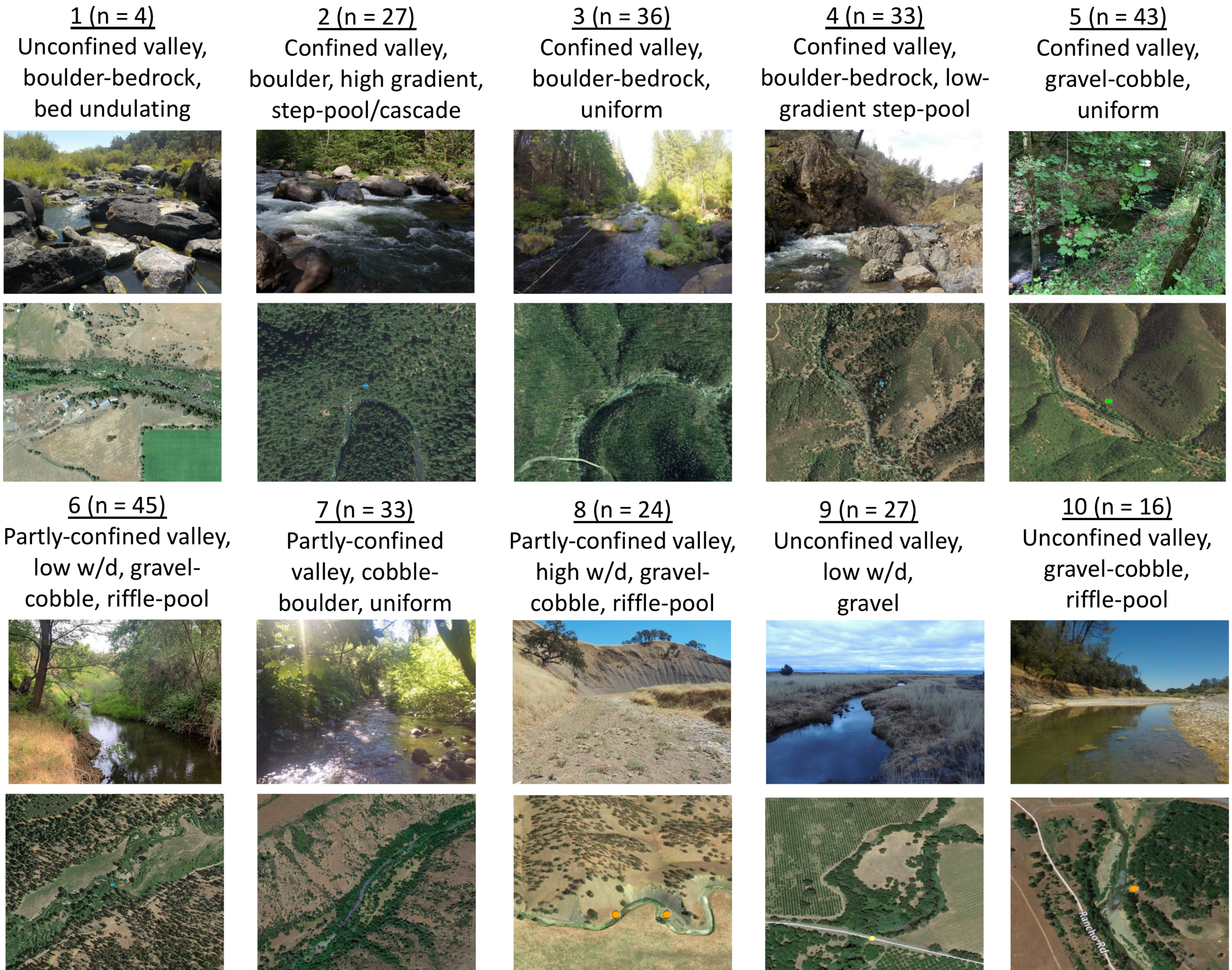
1 (n = 4)
Unconfined valley, boulder-bedrock, bed undulating
2 (n = 27)
Confined valley, boulder, high gradient, step-pool/cascade
3 (n = 36)
Confined valley, boulder-bedrock, uniform
4 (n = 33)
Confined valley, boulder-bedrock, low-gradient step-pool
5 (n = 43)
Confined valley, gravel-cobble, uniform
6 (n = 45)
Partly-confined valley, low w/d, gravel-cobble, riffle-pool
7 (n = 33)
Partly-confined valley, cobble-boulder, uniform
8 (n = 24)
Partly-confined valley, high w/d, gravel-cobble, riffle-pool
9 (n = 27)
Unconfined valley, low w/d, gravel
10 (n = 16)
Unconfined valley, gravel-cobble, riffle-pool

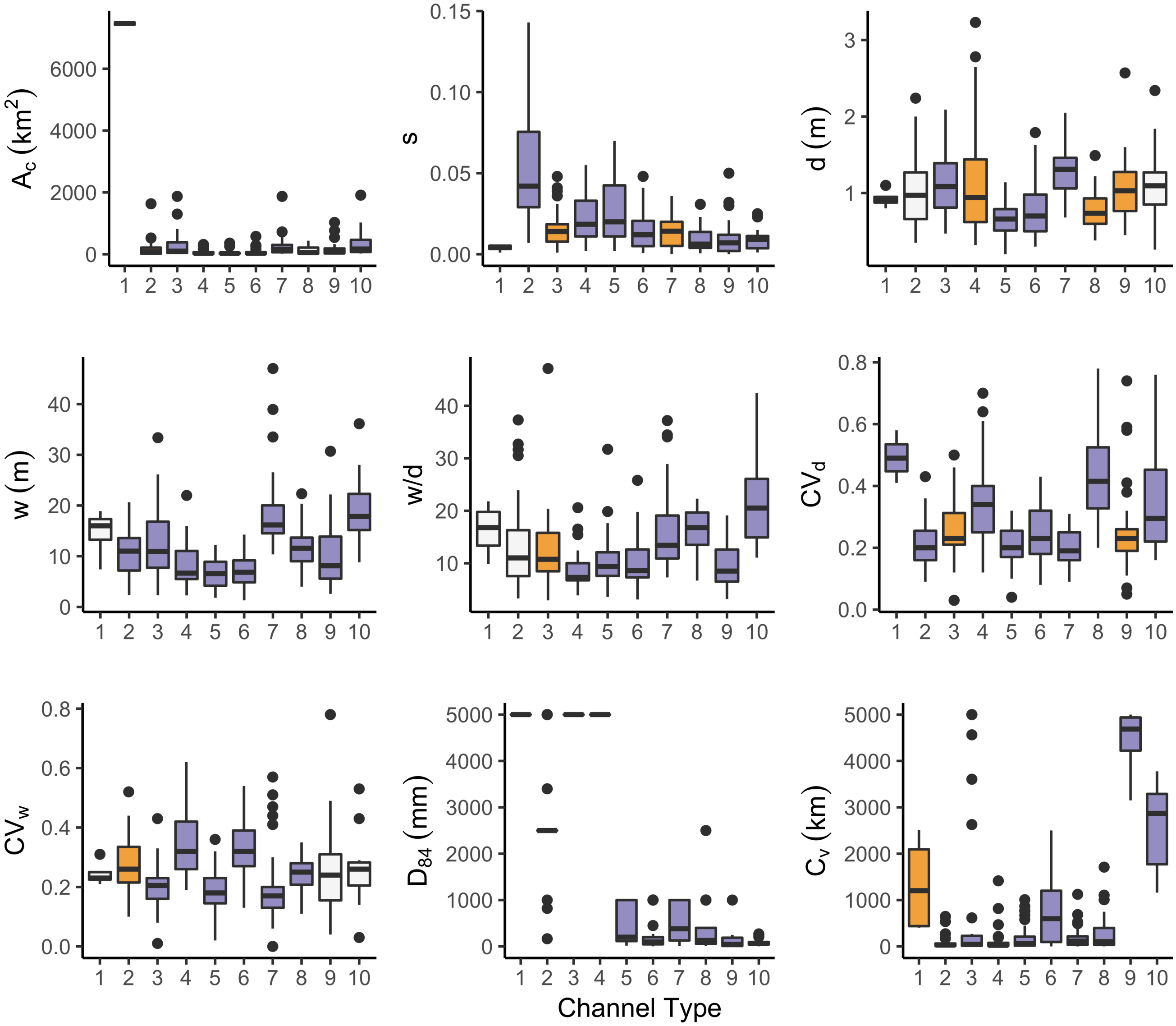

A_c (km^2)
s
d (m)
w (m)
w/d
CV_d
CV_w
D_84 (mm)
C_v (km)
Channel Type

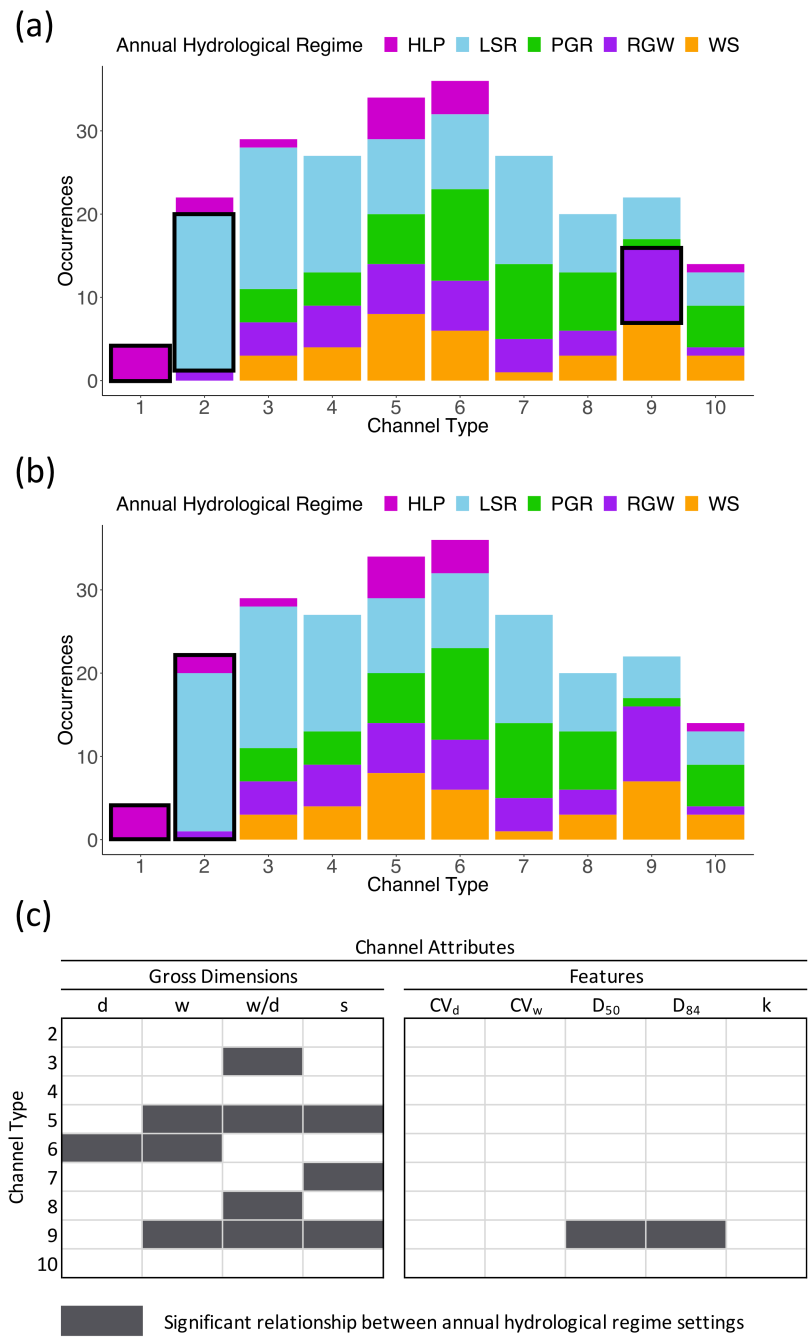
(a)
Annual Hydrological Regime HLP LSR PGR RGW WS
Occurrences
0
10
20
30
1 2 3 4 5 6 7 8 9 10
Channel Type
(b)
Annual Hydrological Regime HLP LSR PGR RGW WS
Occurrences
0
10
20
30
1 2 3 4 5 6 7 8 9 10
Channel Type
(c)
Channel Attributes
Gross Dimensions
Features
d w w/d s
CVd CVw D50 D84 k
Channel Type
2 3 4 5 6 7 8 9 10
Significant relationship between annual hydrological regime settings

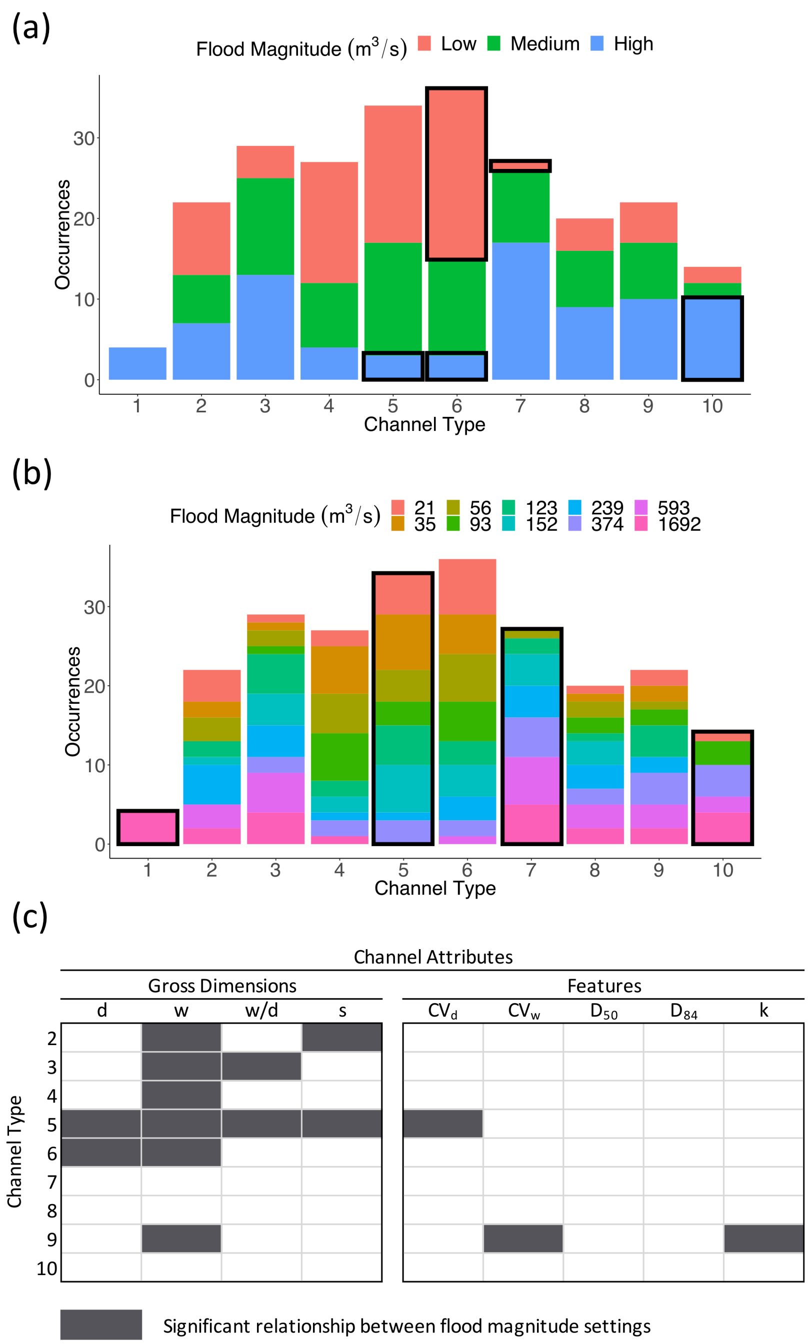
(a)
Flood Magnitude (m3/s) Low Medium High
Occurrences
0 10 20 30
1 2 3 4 5 6 7 8 9 10
Channel Type
(b)
Flood Magnitude (m3/s) 21 35 56 93 123 152 239 374 593 1692
Occurrences
0 10 20 30
1 2 3 4 5 6 7 8 9 10
Channel Type
(c)
Channel Attributes
Gross Dimensions
d w w/d s
Features
CVd CVw D50 D84 k
Channel Type
2 3 4 5 6 7 8 9 10
Significant relationship between flood magnitude settings

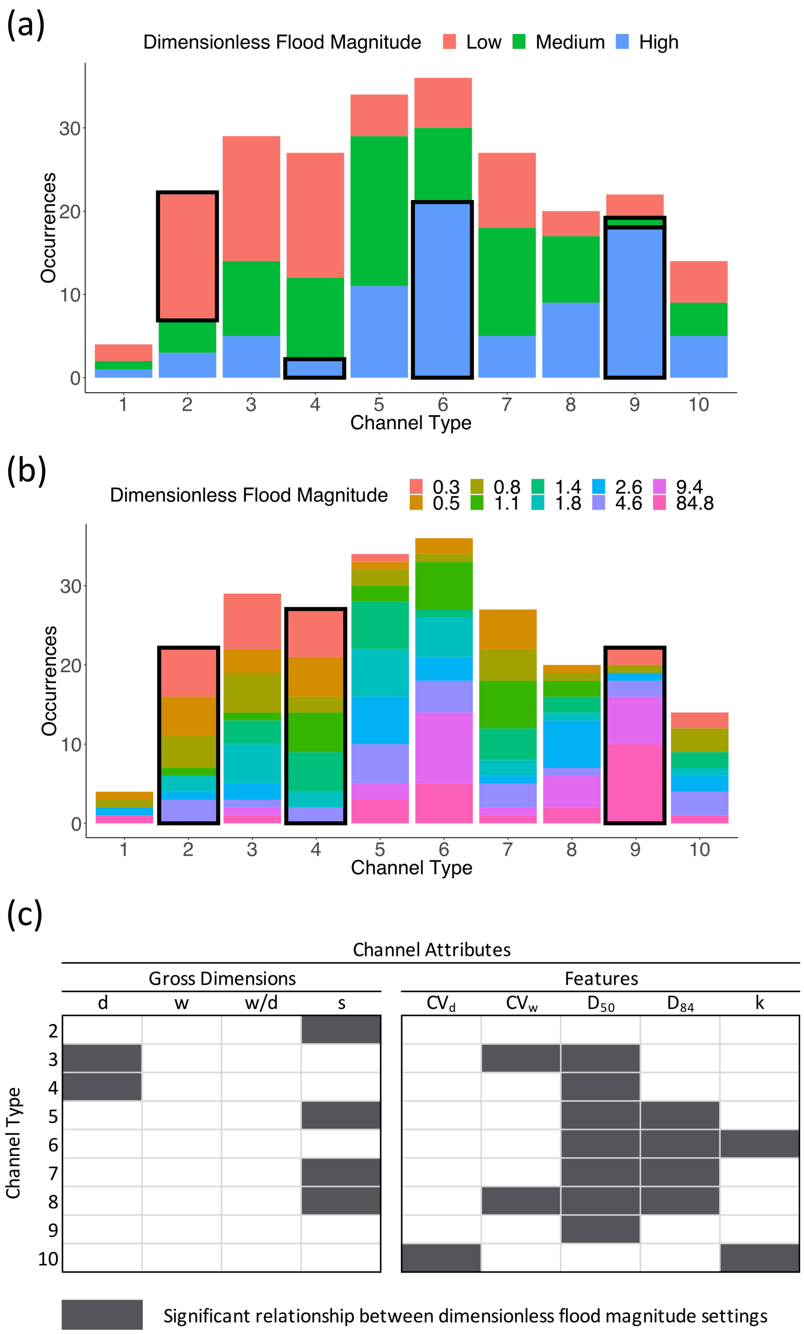
(a)
Dimensionless Flood Magnitude
Low
Medium
High
Occurrences
0
10
20
30
1 2 3 4 5 6 7 8 9 10
Channel Type
(b)
Dimensionless Flood Magnitude
0.3 0.5 0.8 1.1 1.4 1.8 2.6 4.6 9.4 84.8
Occurrences
0
10
20
30
1 2 3 4 5 6 7 8 9 10
Channel Type
(c)
Channel Attributes
Gross Dimensions
Features
d w w/d s
CV$_d$ CV$_w$ D$_{50}$ D$_{84}$ k
Channel Type
2 3 4 5 6 7 8 9 10
Significant relationship between dimensionless flood magnitude settings

Supplementary information to ‘Reach-scale bankfull channel types can exist independently of catchment hydrology’

C.F. Byrne, G.B. Pasternack, H. Guillon, B.A. Lane, S. Sandoval-Solis

Summary statistics of reach-scale sites and channel types

Table S1. Statistical measure of site attributes considered for classification of reach-scale channel types.

	Ac (km^2)	s	d (m)	w (m)	w/d	d/D50	CVd	CVw	k	D50 (mm)	D84 (mm)	Cv (m)
Minimum	1	0.000	0.2	1.3	2.9	0	0.03	0.00	1.01	2	2	1
Maximum	7498	0.143	3.2	47.0	47.1	1285	0.78	0.78	2.20	5000	5000	5000
Range	7497	0.143	3.0	45.7	44.2	1285	0.75	0.78	1.19	4998	4998	4999
Mean	261	0.020	1.0	11.0	12.6	58	0.27	0.25	1.22	249	1733	871
Median	53	0.014	0.9	9.4	10.6	11	0.24	0.24	1.20	70	405	109
Standard Deviation	901	0.020	0.5	6.7	7.1	143	0.13	0.11	0.16	655	2081	1455

Table S2. Median channel attributes considered for classification of reach-scale channel types.

Channel Type	Ac (km^2)	s	d (m)	w (m)	w/d	d/D50	CVd	CVw	k	D50 (mm)	D84 (mm)	Cv (m)
1	7466	0.004	0.9	16.0	16.8	5	0.49	0.23	1.10	564	5000	1202
2	84	0.042	1.0	11.0	11.0	5	0.20	0.26	1.20	250	2500	28
3	100	0.014	1.1	10.9	10.8	6	0.23	0.20	1.20	190	5000	46
4	31	0.018	0.9	6.7	7.3	6	0.34	0.32	1.19	128	5000	23
5	30	0.020	0.7	6.6	9.4	10	0.20	0.18	1.12	57	200	62
6	32	0.012	0.7	6.8	8.6	23	0.23	0.32	1.20	40	95	598
7	164	0.014	1.3	16.2	13.4	16	0.19	0.17	1.23	87	380	114
8	54	0.006	0.7	11.6	16.8	28	0.42	0.25	1.19	27	130	104
9	74	0.007	1.0	8.1	8.5	65	0.23	0.24	1.15	11	45	4688
10	170	0.009	1.1	17.8	20.5	35	0.30	0.26	1.14	28	64	2868

Valley confinement-sediment size relationships

Within the main text of the associated manuscript, statistical relationships between valley confinement distances and sediment size are documented. Figure S1 displays the log-log regressions associated with the statistical metrics in the manuscript.

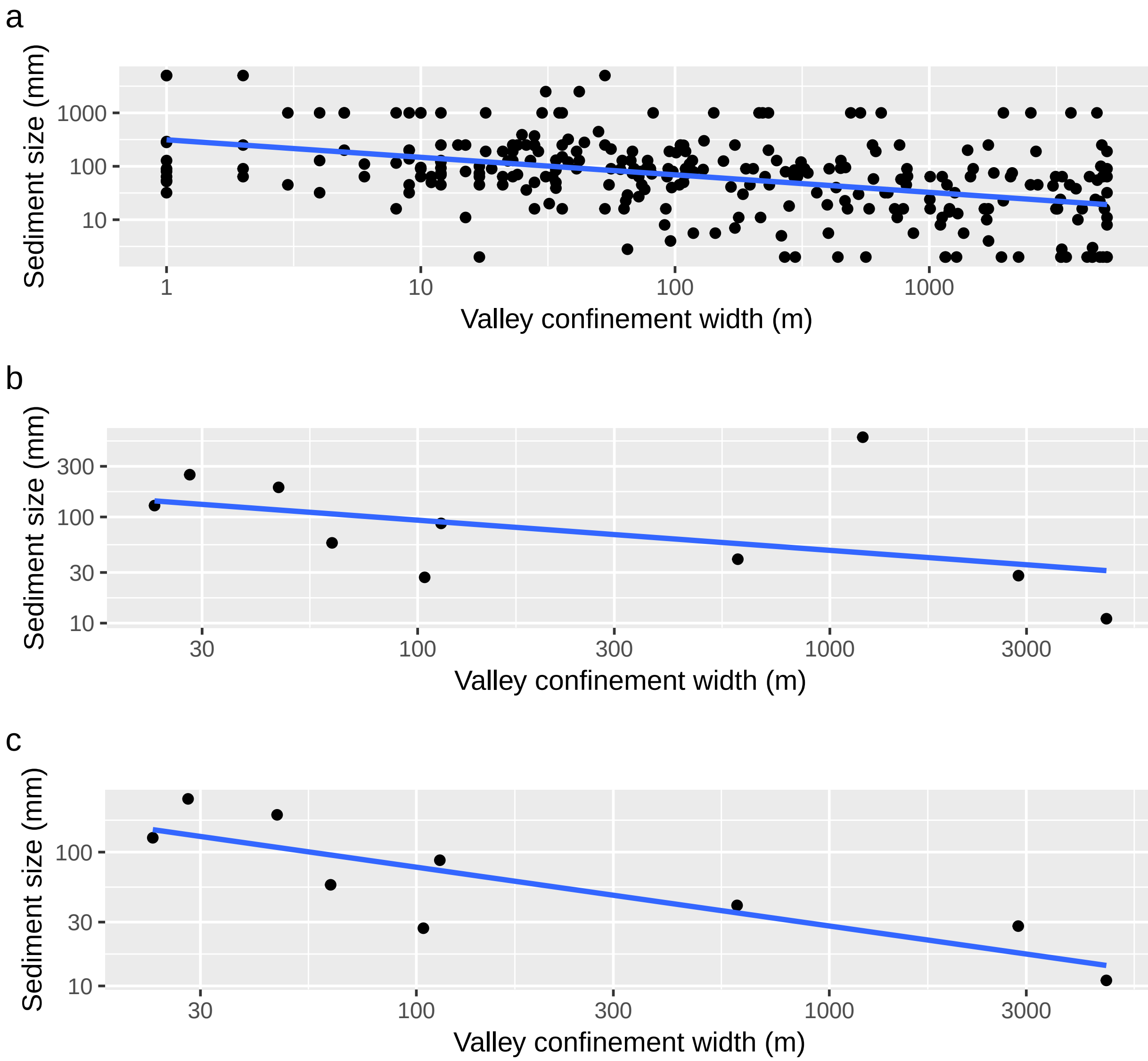

Figure S1. Relationships between valley confinement and sediment size for a) values at all 288 sites, b) median values at all ten channel types, and c) median values for channel types 2 through 10.

Accuracy of reach-scale channel types

Cross-validation of the classification tree was conducted in order to better understand the stability of the multivariate classification. The cross-validation metric is included in the manuscript as it provides the most simple representation of the classification. Two other methods were used to conduct tests of the ability of the classification to predict against unseen data: a multinomial logistic regression implemented with an artificial neural-network (ANN) approach and a generalized linear model (GLM) approach. The ANN approach was implemented using the "multinom" function ('nnet' package) and the GLM appraoch used the "glmnet" function ('glmnet' package). Both functions were run 100 times with a 70-30 percent random subsetting of the classified dataset for training and prediction, respectively. The 100 iterations were conducted to account for sites that may be more or less representative of a channel type and impact the prediction percentage. The average prediction rate of the 100 runs for the ANN and the GLM approaches were 78% and 77%, respectively, which are comparable results to the classification tree cross-validation percentage.

Calculation of site-specific flood discharge

In order to compare reach-scale channel types to flood magnitudes, flows for 2-, 5-, 10-, 25-, and 50-year recurrence interval flood events were estimated at each survey site. These estimations were developed based on the combination of USGS estimations of flow at 84 reference gauges with a minimum of 30-years of flow data and streams binned by defining annual hydrologic regime (Parrett et al., 2011; Lane et al. 2018b). Gauges were binned according to their spatial overlap with binned streams. Contributing area at each gauge location was also estimated using data from 10-m DEM and streamlines from the National Hydrography Dataset Plus Version 2. The binning of gauges by hydrologic regime resulted in notable and consistent differences between gauges in different hydrologic settings, especially high-elevation, low-elevation (HLP) gauges (Fig. S2).

Given the differences in gauge discharge estimates for each of the annual hydrologic regimes, estimation of discharges for all survey sites were also dependent upon the annual hydrologic regime in which it is located. Best-fit power functions were fit to the log-log drainage area-discharge relationships of the following form:

$$Q = kA^m$$

where Q is discharge, A is contributing drainage area, and k and m are numerical constants. Calculated discharges for each site were then used in the comparison of reach-scale channel types with flood magnitude and dimensionless flood magnitude. As discussed in the main text, estimates of flood magnitude for a 10-year recurrence interval were used in the statistal hydrogeomorphic analysis because statistical results were maximized or near maximum. The fit parameters for each of the annual hydrologic regimes at the 10-year recurrence interval are documented in Table S2.

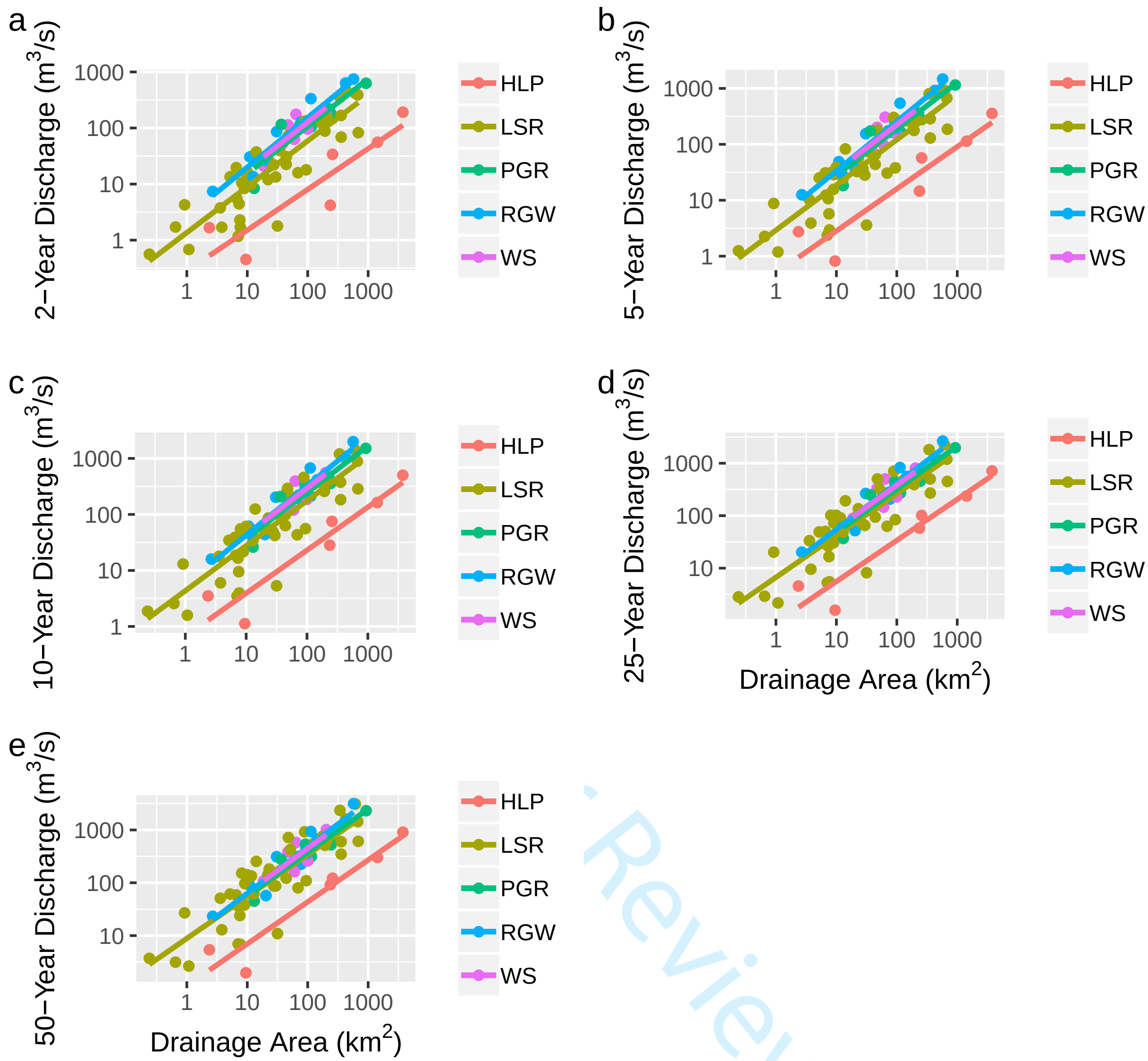

Figure S2. Area-discharge flood regressions for five hydrologic regions within the Sacramento River basin developed from USGS calculated flood magnitudes at reference gauges.

Table S3. Adjusted r-squared values for all log-transformed linear regressions in Figure S2 ($p < 0.05$ for all regressions).

	HLP	LSR	PGR	RGW	WS
TR2si	0.76	0.79	0.80	0.93	0.62
TR5si	0.83	0.78	0.85	0.93	0.61
TR10si	0.86	0.77	0.86	0.93	0.60
TR25si	0.88	0.76	0.88	0.92	0.58
TR50si	0.89	0.75	0.89	0.91	0.56

Site data

Table S4. Reach-scale data for all sites used in geomorphic classification.

	Ac	s	d	w	w/d	d/D50	CVd	CVw	k	D50	D84	Cv	Ls
HLP_518KNCAWC	47	0.041	0.5	13.0	25.8	2.0	0.12	0.42	1.1	247.5	1000.0	108	150
HLP_526CE0323	157	0.029	1.3	7.7	6.1	260.0	0.12	0.44	1.1	5.0	95.0	262	150
HLP_526PS0072	361	0.016	0.7	5.6	7.7	8.2	0.16	0.14	1.2	85.0	756.8	34	750
HLP_526PS0396	71	0.022	0.3	1.9	5.6	6.7	0.37	0.32	1.4	45.0	1000.0	2501	144
HLP_526PS0440	275	0.020	0.7	4.8	7.3	10.8	0.11	0.33	1.2	65.0	270.4	821	150
HLP_526PS1420	76	0.028	0.4	1.3	3.1	20.0	0.19	0.54	1.2	20.0	193.1	32	150
HLP_526PSCBBL	35	0.047	0.5	2.8	6.2	9.6	0.18	0.17	1.1	52.0	1000.0	0	150
HLP_526PSCBLK	14	0.005	0.4	3.3	7.8	200.0	0.08	0.22	1.3	2.0	2.0	1155	150
HLP_526WE0506	275	0.024	0.4	13.7	32.7	1.6	0.43	0.44	1.2	250.0	2500.0	172	150
HLP_526WTCACT	88	0.042	1.3	4.4	3.3	9.4	0.21	0.32	1.4	138.0	3400.0	9	150
HLP_527CE0093	13	0.054	0.4	2.7	6.5	25.0	0.32	0.36	1.3	16.0	250.0	36	298
HLP_527PS0388	32	0.015	0.5	1.8	3.8	17.2	0.18	0.21	1.1	29.0	77.1	65	143
HLP_527PS1156	18	0.042	0.5	2.1	4.4	13.9	0.20	0.27	1.1	36.0	111.0	26	150
HLP_527PS1412	25	0.043	0.6	2.4	4.0	22.2	0.17	0.16	1.3	27.0	146.8	72	150
HLP_527SED084	44	0.007	0.3	4.3	17.2	30.0	0.28	0.23	1.1	10.0	40.0	1682	293
HLP_3	45	0.010	0.3	8.8	33.7	0.1	0.21	0.03	1.7	2.8	5.6	3320	150
HLP_4	1030	0.020	1.3	10.5	12.9	0.1	0.05	0.22	1.1	11.0	190.0	5000	150
HLP_10	71	0.039	1.2	10.6	8.6	6.3	0.25	0.24	1.2	190.0	5000.0	616	150
HLP_24	44	0.007	0.4	16.0	37.3	0.4	0.11	0.26	1.3	1000.0	5000.0	536	150
HLP_28	233	0.003	0.5	23.1	47.1	2.6	0.28	0.43	1.2	190.0	5000.0	5000	150
HLP_37	591	0.012	0.9	8.2	8.9	4.7	0.12	0.29	1.4	190.0	5000.0	2628	150
HLP_53	7498	0.006	0.9	16.8	19.1	0.9	0.46	0.20	1.1	1000.0	5000.0	2509	150
HLP_54	7498	0.005	0.9	18.9	21.8	0.9	0.41	0.23	1.3	1000.0	5000.0	1956	250
HLP_55	7434	0.004	1.1	15.2	14.5	8.2	0.58	0.21	1.1	128.0	5000.0	449	150
HLP_59	7398	0.001	0.8	7.4	9.9	8.3	0.52	0.31	1.1	90.0	5000.0	404	150
LSR_504PS0227	544	0.009	1.6	30.7	19.1	16.0	0.25	0.31	1.3	100.0	250.0	4728	250
LSR_505BMCMCR	4	0.098	0.7	7.3	10.0	2.6	0.20	0.35	1.2	280.0	820.0	44	150
LSR_505CE0137	31	0.032	1.1	3.7	3.7	66.0	0.23	0.35	1.1	16.0	250.0	3150	148
LSR_505LBCAMR	9	0.143	0.9	7.1	8.7	2.2	0.22	0.28	1.2	390.0	2500.0	25	150
LSR_505PS0156	624	0.018	1.5	15.7	10.9	27.1	0.10	0.14	1.8	54.0	1000.0	0	250
LSR_505PS1180	187	0.023	1.1	14.1	16.3	15.1	0.53	0.27	1.7	75.0	205.0	2119	300
LSR_507CE0581	84	0.048	0.7	9.1	14.4	2.7	0.19	0.28	1.2	250.0	2500.0	14	198
LSR_507MZCAML	20	0.075	1.0	6.4	6.9	24.8	0.19	0.27	1.2	39.0	165.0	34	150
LSR_507PS0122	366	0.017	1.3	11.4	12.6	25.6	0.25	0.26	1.2	50.0	2500.0	108	150
LSR_507PS0286	6	0.076	0.4	2.3	5.8	5.6	0.26	0.42	1.1	79.0	2500.0	272	134
LSR_507PS0314	488	0.020	2.0	10.9	5.7	8.0	0.22	0.13	1.3	250.0	2500.0	28	150
LSR_507SHA915	68	0.048	1.1	9.5	8.7	17.2	0.29	0.17	1.4	64.0	5000.0	226	150
LSR_507WE0988	21	0.028	0.4	6.8	19.8	1.4	0.23	0.24	1.2	250.0	1000.0	1707	150
LSR_509ACNFPP	108	0.027	1.3	12.7	10.0	12.2	0.26	0.15	1.1	110.0	1000.0	114	600
LSR_509ACSFPP	119	0.028	1.5	16.6	11.2	18.6	0.18	0.44	1.2	80.0	1000.0	112	150
LSR_509ATCINC	231	0.017	1.2	16.2	13.4	14.0	0.11	0.06	1.3	87.0	1000.0	129	150
LSR_509BCCH32	48	0.026	1.3	11.7	9.4	10.1	0.18	0.20	1.1	130.0	1000.0	34	150
LSR_509BSCADC	22	0.048	0.7	6.7	10.0	3.5	0.17	0.19	1.2	200.0	1000.0	9	150
LSR_509CBCADC	16	0.079	1.3	7.4	6.1	1.3	0.20	0.22	1.5	1000.0	5000.0	30	150
LSR_509CTCADC	5	0.016	0.5	4.4	8.4	255.5	0.22	0.52	1.5	2.0	20.0	17	150

Table S4 (cont'd). Reach-scale data for all sites used in geomorphic classification (cont'd).

	Ac	s	d	w	w/d	d/D50	CVd	CVw	k	D50	D84	Cv	Ls
LSR_509DCPWxx	439	0.021	1.5	22.3	18.5	1.5	0.69	0.25	1.3	1000	2500	35	250
LSR_509DRCBPC	316	0.028	1.2	21.5	19.1	3.9	0.15	0.19	1.2	300	1000	130	250
LSR_509ICPPCX	261	0.044	1.0	8.3	9.7	12.0	0.20	0.25	1.3	79	1000	118	300
LSR_509PS0049	79	0.015	1.2	39.0	34.5	579.1	0.31	0.47	1.5	2	64	437	285
LSR_509PS0085	132	0.042	1.8	20.6	12.6	7.1	0.22	0.26	1.3	250	2500	12	240
LSR_509PS0170	22	0.034	0.8	7.4	9.8	15.5	0.16	0.23	1.1	50	350	34	150
LSR_509PS0234	261	0.016	1.1	15.5	15.1	5.2	0.27	0.11	1.3	210	1000	56	500
LSR_514DNCLDC	24	0.036	1.0	9.7	10.9	1.0	0.21	0.23	1.2	1000	5000	10	150
LSR_514PS0099	500	0.015	2.1	25.6	13.7	5.6	0.35	0.23	1.2	370	5000	28	250
LSR_514SED078	76	0.011	0.7	20.8	28.9	11.3	0.19	0.15	1.3	64	250	1124	250
LSR_517LCCAYB	12	0.022	0.4	4.3	12.7	5.6	0.39	0.38	1.2	75	190	333	143
LSR_517PS0054	56	0.047	1.8	14.6	9.3	1.2	0.29	0.30	1.4	2500	5000	42	150
LSR_517PS0061	18	0.053	1.7	9.9	6.9	6.8	0.35	0.42	1.3	250	5000	105	150
LSR_517PS0074	25	0.042	1.1	12.2	11.1	6.3	0.19	0.20	1.2	180	1000	101	150
LSR_517WE0515	375	0.007	0.8	13.4	18.8	3.1	0.22	0.33	1.3	250	5000	15	150
LSR_518BTCASC	53	0.025	0.7	10.7	14.7	8.3	0.21	0.14	1.1	90	315	323	150
LSR_518CE0015	460	0.013	0.9	20.0	23.7	3.5	0.24	0.14	1.3	250	1000	36	425
LSR_518CE0034	64	0.020	0.9	14.4	17.1	3.6	0.24	0.17	1.4	250	1000	53	277
LSR_518CE0047	34	0.025	0.3	10.6	42.5	4.0	0.22	0.29	1.2	64	250	3140	148
LSR_518CE0114	1633	0.052	1.1	14.3	14.7	4.2	0.21	0.27	1.4	250	2500	26	376
LSR_518CE0242	26	0.015	0.5	9.8	19.9	7.8	0.10	0.04	1.4	64	64	1008	148
LSR_518CE0338	4	0.106	1.2	9.3	8.3	15.9	0.12	0.36	1.1	72	1000	81	150
LSR_518CE0543	238	0.005	0.5	12.3	26.6	230.0	0.21	0.21	1.1	2	2	3455	148
LSR_518CE0575	21	0.006	0.5	3.0	5.9	270.0	0.19	0.42	1.3	2	16	3302	141
LSR_518CE0879	1911	0.008	1.5	20.0	14.9	725.0	0.29	0.26	1.2	2	16	1160	198
LSR_518CE0895	2	0.013	1.0	8.5	8.3	64.6	0.24	0.24	1.5	16	64	3993	148
LSR_518CPCRCR	46	0.044	2.2	13.5	6.5	18.7	0.34	0.19	1.4	120	2500	38	300
LSR_518GZCUPx	35	0.013	1.0	13.1	15.3	13.5	0.35	0.25	1.4	71	1000	110	450
LSR_518PS0017	61	0.015	0.9	16.1	20.4	7.4	0.39	0.14	1.3	120	5000	12	150
LSR_518PS0029	526	0.040	1.2	12.4	11.0	3.7	0.29	0.37	1.2	320	2500	38	300
LSR_518PS0033	5	0.091	0.7	6.6	9.4	9.7	0.20	0.26	1.2	74	5000	12	143
LSR_518PS0045	11	0.052	0.5	5.5	12.4	1.7	0.29	0.49	1.3	280	5000	0	135
LSR_518PS0089	29	0.005	0.3	6.2	18.8	170.0	0.15	0.32	1.1	2	2	563	285
LSR_518PS0093	70	0.049	0.6	10.3	17.6	8.3	0.20	0.13	1.3	74	430	68	150
LSR_518PS0113	34	0.049	1.1	11.6	10.6	9.0	0.20	0.26	1.1	126	1000	22	150
LSR_518PS0125	1872	0.013	1.5	19.8	13.1	22.1	0.16	0.30	1.3	69	1000	12	250
LSR_518RCNAPC	27	0.024	1.2	17.2	14.9	16.2	0.22	0.28	1.3	75	270	1794	150
LSR_518SDCAHR	65	0.011	0.7	4.9	6.6	30.6	0.20	0.37	1.4	24	69	1005	150
LSR_518SED013	53	0.012	0.7	9.5	14.6	11.2	0.21	0.43	1.3	58	250	603	150
LSR_518SED015	60	0.005	0.6	13.6	21.2	33.7	0.20	0.21	1.1	19	73	397	250
LSR_518SED082	20	0.004	0.8	13.1	17.5	107.1	0.60	0.21	1.1	7	64	172	150
LSR_518SED086	50	0.032	1.0	10.8	11.6	10.5	0.29	0.17	1.4	95	2500	10	300
LSR_518SED089	30	0.011	0.2	6.0	31.7	4.9	0.29	0.09	2.0	40	150	430	150
LSR_518SED091	38	0.011	0.5	8.8	17.9	30.6	0.51	0.28	1.1	16	64	1008	150
LSR_518SNCABC	52	0.028	0.5	4.0	7.8	17.4	0.18	0.30	1.1	30	97	185	143

Table S4 (cont'd). Reach-scale data for all sites used in geomorphic classification (cont'd).

	Ac	s	d	w	w/d	d/D50	CVd	CVw	k	D50	D84	Cv	Ls
LSR_518WE0521	60	0.020	1.4	14.9	10.9	15.9	0.17	0.23	1.3	88	310	61	150
LSR_518WLCBCP	24	0.031	0.4	1.6	4.0	30.9	0.24	0.39	1.2	13	49	1294	128
LSR_518WLCBWL	20	0.036	0.7	25.0	37.2	38.0	0.14	0.00	1.1	18	91	281	143
LSR_518YLCAFR	199	0.030	1.9	16.8	10.5	6.6	0.44	0.22	1.7	290	5000	0	250
LSR_521BTCLBC	305	0.014	0.9	8.5	9.2	470.5	0.14	0.08	1.2	2	5000	270	250
LSR_522GSCBSC	262	0.018	0.6	11.5	22.0	11.8	0.36	0.26	1.3	50	120	28	150
LSR_522MFSCRB	83	0.021	0.8	9.1	11.8	18.1	0.21	0.15	1.4	45	1000	21	150
LSR_522PS0430	247	0.030	1.1	14.5	13.9	11.7	0.18	0.13	1.4	93	1000	12	250
LSR_522WE0767	36	0.015	0.4	7.4	20.6	6.1	0.21	0.36	1.3	64	5000	21	150
LSR_523PS0172	9	0.075	1.0	5.3	5.3	9.2	0.09	0.24	1.2	110	2500	6	150
LSR_523PS0414	67	0.041	1.2	9.3	8.7	18.5	0.22	0.22	1.3	64	5000	6	150
LSR_523TMCATG	409	0.041	0.7	15.5	23.9	5.7	0.12	0.15	1.3	115	2500	8	150
LSR_523WE0512	67	0.029	0.4	6.8	20.7	5.4	0.20	0.21	1.4	64	2500	0	150
LSR_526CE0341	90	0.050	0.8	11.8	17.5	0.8	0.31	0.22	1.2	1000	2500	12	200
LSR_526CE0483	9	0.070	0.5	4.7	11.3	7.8	0.25	0.28	1.3	57	520	774	298
LSR_526PS0220	469	0.019	1.3	18.6	14.3	1.3	0.18	0.14	2.2	1000	1000	491	250
LSR_526PS0356	767	0.001	1.3	8.1	6.4	655.0	0.22	0.49	1.4	2	26	4820	150
LSR_526WE0744	154	0.026	0.4	11.2	31.6	0.2	0.14	0.26	1.2	2500	2500	31	150
LSR_0	298	0.002	0.7	18.4	25.2	11.4	0.27	0.14	1.1	64	90	3331	250
LSR_1	15	0.003	1.4	10.0	7.3	85.1	0.33	0.39	1.1	16	32	477	150
LSR_2	86	0.005	0.8	10.1	13.1	17.1	0.23	0.18	1.1	45	90	1174	150
LSR_5	101	0.050	0.8	6.6	8.5	17.2	0.18	0.20	1.3	45	90	3566	250
LSR_6	46	0.011	0.5	5.1	9.8	185.1	0.38	0.31	1.1	3	45	4386	150
LSR_7	1299	0.011	0.8	14.9	18.1	0.8	0.34	0.15	1.2	1000	5000	8	250
LSR_8	4	0.024	0.4	6.5	15.6	6.5	0.18	0.31	1.1	64	190	294	250
LSR_9	221	0.006	0.6	7.2	12.7	6.3	0.22	0.17	1.0	90	5000	5000	150
LSR_11	78	0.031	0.5	6.6	14.2	0.5	0.50	0.27	1.1	1000	5000	3606	150
LSR_12	4	0.026	0.9	3.5	3.9	7.0	0.24	0.27	1.1	128	5000	67	250
LSR_13	21	0.008	0.3	5.3	16.5	2.5	0.18	0.23	1.0	128	5000	78	150
LSR_14	148	0.033	1.8	14.8	8.1	1.8	0.12	0.51	1.3	1000	5000	10	250
LSR_15	11	0.033	0.6	5.9	10.4	12.5	0.29	0.24	1.2	45	5000	74	150
LSR_16	14	0.008	0.6	4.8	8.7	6.2	0.41	0.37	1.1	90	5000	80	150
LSR_17	33	0.016	0.9	6.4	6.8	0.9	0.21	0.62	1.1	1000	5000	214	150
LSR_18	181	0.008	1.0	16.0	15.4	8.1	0.60	0.25	1.1	128	5000	42	250
LSR_20	6	0.015	0.6	4.3	6.9	6.3	0.61	0.35	1.1	90	5000	10	150
LSR_21	8	0.024	0.4	2.3	6.4	4.0	0.64	0.29	1.1	90	5000	77	150
LSR_22	36	0.033	0.7	7.7	11.0	7.8	0.25	0.33	1.2	90	5000	190	250
LSR_23	13	0.026	1.3	7.7	5.9	1.3	0.18	0.20	1.1	1000	5000	4	150
LSR_25	733	0.016	0.8	2.3	2.9	0.8	0.46	0.14	1.2	1000	5000	4564	250
LSR_29	52	0.008	0.6	5.8	9.9	6.5	0.32	0.20	1.0	90	5000	203	150
LSR_32	821	0.010	1.9	33.4	17.5	1.9	0.23	0.21	1.1	1000	5000	82	250
LSR_34	1872	0.001	1.2	16.9	14.1	18.7	0.26	0.20	1.2	64	5000	33	250
LSR_36	250	0.006	0.7	14.0	20.3	10.8	0.40	0.35	1.4	64	190	17	250
LSR_38	288	0.017	0.7	9.2	13.4	10.2	0.35	0.43	1.1	90	190	34	250
LSR_40	123	0.015	1.5	17.3	11.4	1.5	0.21	0.24	1.1	1000	5000	142	150

Table S4 (cont'd). Reach-scale data for all sites used in geomorphic classification (cont'd).

	Ac	s	d	w	w/d	d/D50	CVd	CVw	k	D50	D84	Cv	Ls
LSR_41	417	0.0090	1.4	26.1	18.8	7.3	0.23	0.09	1.1	190.0	5000.0	68	250
LSR_42	723	0.0030	1.2	33.5	28.5	26.1	0.19	0.06	1.1	45.0	128.0	197	250
LSR_43	182	0.0040	0.7	6.3	8.6	11.5	0.38	0.41	1.4	64.0	5000.0	10	150
LSR_44	98	0.0280	0.8	11.7	15.1	4.1	0.15	0.10	1.0	190.0	2500.0	110	150
LSR_45	821	0.0010	1.5	24.1	15.7	12.0	0.41	0.22	1.2	128.0	5000.0	0	250
LSR_46	196	0.0090	0.7	13.1	18.5	7.9	0.24	0.20	1.2	90.0	5000.0	110	250
LSR_47	633	0.0080	1.1	19.1	17.1	1.1	0.21	0.31	1.2	1000.0	5000.0	36	250
LSR_48	312	0.0010	0.6	10.6	18.5	35.7	0.29	0.25	1.3	16.0	32.0	8	250
LSR_49	371	0.0300	0.6	18.2	30.5	0.6	0.36	0.52	1.2	1000.0	5000.0	9	250
LSR_50	47	0.0180	0.7	7.2	10.6	5.3	0.25	0.16	1.1	128.0	5000.0	251	150
PGR_0	14	0.0006	0.7	4.8	6.7	89.6	0.45	0.16	1.1	8.0	22.6	1106	150
PGR_2	221	0.0001	1.5	10.7	7.3	132.5	0.11	0.17	1.1	11.0	22.6	178	150
PGR_3	90	0.0040	2.1	47.0	22.9	64.0	0.21	0.57	1.1	32.0	64.0	687	250
PGR_4	47	0.0065	0.7	10.3	14.4	44.8	0.41	0.18	1.2	16.0	64.0	53	150
PGR_5	32	0.0107	0.7	6.1	9.2	10.4	0.30	0.34	1.2	64.0	90.0	1452	150
PGR_6	246	0.0041	1.5	18.4	12.7	11.4	0.19	0.20	1.2	128.0	200.0	117	250
PGR_7	48	0.0118	0.8	10.9	13.4	51.0	0.26	0.16	1.1	16.0	128.0	28	150
PGR_8	168	0.0150	2.8	13.9	5.0	0.7	0.23	0.19	1.1	5000.0	5000.0	2	150
PGR_9	48	0.0090	0.7	9.7	13.6	64.5	0.24	0.13	1.2	11.0	90.0	15	150
PGR_10	67	0.0043	0.8	9.5	11.7	101.8	0.58	0.20	1.5	8.0	64.0	91	150
PGR_11	19	0.0126	0.7	8.4	11.9	15.6	0.19	0.27	1.1	45.0	128.0	55	150
PGR_12	32	0.0109	0.7	5.2	7.5	10.7	0.14	0.18	1.1	64.0	190.0	2	150
PGR_13	6	0.0023	1.1	4.6	4.1	12.4	0.26	0.42	1.1	90.0	5000.0	1	150
PGR_14	101	0.0088	1.6	14.6	9.5	24.2	0.25	0.19	1.3	64.0	1000.0	23	150
PGR_15	6	0.0153	0.7	5.3	7.3	0.2	0.20	0.42	1.2	5000.0	5000.0	0	150
PGR_16	245	0.0206	0.6	7.1	11.0	10.1	0.27	0.27	1.1	64.0	200.0	31	150
PGR_17	164	0.0051	1.0	15.3	15.3	91.3	0.25	0.18	1.2	11.0	22.6	217	150
PGR_18	10	0.0027	1.5	6.9	4.7	1.5	0.20	0.23	1.2	1000.0	5000.0	5	150
PGR_19	398	0.0002	1.1	14.5	13.1	12.3	0.26	0.17	1.5	90.0	190.0	10	250
PGR_20	52	0.0107	1.4	12.9	9.2	31.2	0.15	0.13	1.6	45.0	1000.0	104	150
PGR_21	16	0.0005	1.3	10.4	7.7	7.1	0.27	0.13	1.2	190.0	1000.0	21	150
PGR_22	38	0.0053	0.8	10.4	13.1	24.7	0.27	0.22	1.1	32.0	128.0	4	150
PGR_23	8	0.0007	0.8	6.3	7.6	51.5	0.15	0.13	1.3	16.0	32.0	790	150
PGR_24	5	0.0058	0.4	3.3	9.3	11.2	0.37	0.49	1.2	32.0	64.0	361	150
PGR_25	971	0.0011	0.9	23.0	25.9	27.7	0.43	0.53	1.1	32.0	64.0	1260	150
PGR_26	220	0.0011	1.5	15.0	10.2	261.4	0.21	0.19	1.1	5.6	11.0	118	150
PGR_27	6	0.0050	0.7	4.4	6.5	15.2	0.12	0.37	1.1	45.0	200.0	9	150
PGR_28	1025	0.0091	1.1	20.9	19.1	24.3	0.37	0.29	1.2	45.0	90.0	2671	250
PGR_29	43	0.0084	1.3	10.3	8.1	637.3	0.30	0.38	1.8	2.0	45.0	1280	150
PGR_30	34	0.0003	0.5	2.6	5.4	240.5	0.17	0.24	1.2	2.0	8.0	4986	150
PGR_31	317	0.0185	0.9	6.5	7.3	19.8	0.34	0.44	1.3	45.0	5000.0	12	150
PGR_32	5	0.0014	0.9	6.1	6.7	14.1	0.38	0.19	1.1	64.0	200.0	303	150
PGR_33	17	0.0140	0.9	7.0	7.5	234.6	0.43	0.28	1.2	4.0	32.0	96	150
PGR_34	23	0.0039	1.1	23.6	21.4	49.0	0.28	0.25	1.1	22.6	64.0	1955	250
PGR_35	19	0.0033	0.7	5.6	8.6	40.5	0.34	0.43	1.3	16.0	45.0	1201	150

Table S4 (cont'd). Reach-scale data for all sites used in geomorphic classification (cont'd).

	Ac	s	d	w	w/d	d/D50	CVd	CVw	k	D50	D84	Cv	Ls
PGR_36	11	0.0048	1.2	9.2	7.7	74.1	0.34	0.33	1.1	16.0	90.0	92	150
PGR_37	21	0.0054	1.4	7.7	5.6	7.3	0.21	0.21	1.2	190.0	5000.0	23	150
PGR_38	3	0.0308	0.6	4.0	6.7	4.7	0.60	0.25	1.1	128.0	1000.0	12	150
PGR_41	46	0.0143	0.9	6.6	7.4	4.7	0.22	0.18	1.3	190.0	5000.0	41	150
PGR_42	42	0.0025	0.8	7.3	9.4	17.3	0.31	0.35	1.4	45.0	200.0	3	150
PGR_43	48	0.0057	0.9	11.7	12.7	10.2	0.35	0.29	1.2	90.0	200.0	69	150
PGR_44	135	0.0013	1.1	15.5	14.1	68.8	0.30	0.26	1.1	16.0	32.0	1647	150
PGR_45	204	0.0014	1.0	9.1	9.1	250.5	0.57	0.17	1.1	4.0	11.0	1710	150
PGR_47	1027	0.0092	1.0	28.0	28.0	62.4	0.44	0.21	1.1	16.0	45.0	3193	250
PGR_509BCCBPW	164	0.0142	0.7	16.9	23.6	5.8	0.27	0.07	1.3	125.0	1000.0	155	250
PGR_513PS0024	26	0.0280	3.2	14.2	4.4	50.4	0.30	0.19	1.2	64.0	5000.0	11	250
PGR_504CE0210	193	0.0155	1.6	15.1	10.0	6.4	0.26	0.16	1.1	250.0	250.0	4771	250
PGR_508PS0458	614	0.0240	0.8	26.6	34.1	27.3	0.19	0.11	1.0	30.0	79.0	527	250
PGR_513PS0088	577	0.0185	0.9	10.2	12.1	23.1	0.20	0.32	1.1	40.0	95.0	97	250
PGR_513PS0200	96	0.0155	0.8	9.0	12.3	22.1	0.31	0.19	1.3	37.0	115.0	76	150
PGR_524PS0202	299	0.0070	1.1	20.4	20.8	26.1	0.34	0.21	1.1	41.0	140.0	166	250
PGR_513PS0248	62	0.0200	0.6	7.8	15.1	7.9	0.26	0.10	1.1	70.0	240.0	24	150
PGR_524SHA916	271	0.0150	1.7	12.5	7.5	16.5	0.27	0.17	1.2	80.0	5000.0	73	250
PGR_513BTCACC	46	0.0260	0.5	5.5	12.4	5.0	0.34	0.26	1.2	100.0	5000.0	17	150
RGW_0	8	0.0260	0.9	5.8	6.9	0.9	0.39	0.30	1.3	1000.0	5000.0	3	150
RGW_1	6	0.0230	0.4	5.3	13.8	12.1	0.51	0.28	1.1	32.0	200.0	1	150
RGW_2	37	0.0060	0.8	8.8	11.3	6.1	0.32	0.10	1.1	128.0	200.0	62	150
RGW_3	40	0.0090	1.1	18.1	16.2	5.9	0.14	0.21	1.4	190.0	5000.0	95	250
RGW_4	241	0.0030	1.8	36.1	19.6	115.0	0.63	0.19	1.1	16.0	45.0	1707	250
RGW_5	5	0.0110	0.4	3.4	8.1	9.2	0.20	0.22	1.1	45.0	90.0	235	150
RGW_6	35	0.0035	0.4	7.4	19.6	34.5	0.42	0.23	1.2	11.0	16.0	748	150
RGW_7	5	0.0060	1.2	15.1	12.4	1.2	0.78	0.32	1.3	1000.0	1000.0	233	150
RGW_8	197	0.0030	1.3	13.2	10.5	39.2	0.19	0.22	1.2	32.0	64.0	5000	250
RGW_9	263	0.0020	2.1	22.0	10.7	16.1	0.24	0.44	1.2	128.0	5000.0	4	250
RGW_10	22	0.0090	0.8	11.2	14.3	0.8	0.28	0.31	1.3	1000.0	1000.0	221	150
RGW_11	52	0.0060	1.1	14.6	13.8	66.2	0.27	0.51	1.1	16.0	64.0	63	150
RGW_12	7	0.0080	0.5	3.1	6.7	14.5	0.18	0.16	1.0	32.0	128.0	9	150
RGW_15	97	0.0080	0.8	9.4	12.3	47.7	0.20	0.15	1.1	16.0	32.0	4889	150
RGW_16	97	0.0010	1.3	12.2	9.2	29.5	0.21	0.25	1.1	45.0	200.0	812	150
RGW_18	41	0.0370	1.4	9.9	7.1	0.4	0.34	0.32	1.3	5000.0	5000.0	0	150
RGW_23	79	0.0030	0.8	6.7	8.8	8.4	0.42	0.25	1.3	90.0	5000.0	817	150
RGW_27	10	0.0030	0.7	4.6	6.4	129.7	0.17	0.15	1.3	5.6	16.0	1365	150
RGW_29	195	0.0020	1.0	11.6	11.5	5.3	0.31	0.10	1.2	190.0	5000.0	18	150
RGW_31	181	0.0010	1.0	16.1	15.6	128.9	0.24	0.10	1.3	8.0	32.0	5000	250
RGW_36	327	0.0040	0.9	15.1	17.5	13.4	0.23	0.25	1.1	64.0	128.0	4269	250
RGW_37	136	0.0040	1.3	9.9	7.6	118.8	0.23	0.20	1.4	11.0	22.6	1124	150
RGW_41	43	0.0200	1.4	8.7	6.3	6.9	0.21	0.21	1.0	200.0	5000.0	233	150
RGW_42	40	0.0020	1.0	9.4	9.5	15.5	0.30	0.15	1.3	64.0	200.0	93	250
RGW_43	31	0.0200	1.0	11.7	11.6	5.3	0.32	0.16	1.1	190.0	5000.0	29	150
RGW_44	7	0.0130	1.1	7.2	6.7	0.3	0.35	0.35	1.6	5000.0	5000.0	53	150

Table S4 (cont'd). Reach-scale data for all sites used in geomorphic classification (cont'd).

	Ac	s	d	w	w/d	d/D50	CVd	CVw	k	D50	D84	Cv	Ls
RGW_45	4	0.0200	0.5	6.8	12.6	6.0	0.31	0.39	1.2	90.0	1000.0	41	150
RGW_46	9	0.0270	0.7	6.6	9.4	15.5	0.10	0.18	1.0	45.0	128.0	17	150
RGW_47	40	0.0070	1.2	12.4	10.4	13.2	0.18	0.29	1.1	90.0	200.0	1488	250
RGW_48	4	0.0060	0.6	5.5	8.9	0.6	0.16	0.19	1.1	1000.0	1000.0	5	150
RGW_50	8	0.0080	0.8	16.3	20.0	4.1	0.27	0.22	1.2	200.0	1000.0	9	250
RGW_51	52	0.0100	1.3	11.0	8.9	6.2	0.40	0.31	1.1	200.0	5000.0	1415	150
RGW_507CE0181	27	0.0200	0.6	4.1	7.6	2.2	0.21	0.24	1.1	250.0	1000.0	764	150
RGW_520CE0562	87	0.0110	1.4	11.0	8.2	21.2	0.11	0.04	1.2	64.0	250.0	4808	250
RGW_509PCDTWR	21	0.0250	1.1	7.2	6.6	17.4	0.16	0.11	1.0	64.0	115.0	72	150
RGW_514CE0139	39	0.0270	0.6	8.2	15.4	2.2	0.36	0.40	1.2	250.0	1000.0	598	150
RGW_514PS0351	37	0.0150	1.3	17.1	13.3	10.9	0.09	0.18	1.1	120.0	380.0	313	250
RGW_513PS0008	19	0.0290	1.2	9.1	8.6	14.7	0.37	0.29	1.2	80.0	1000.0	0	150
RGW_513STCAIV	8	0.0480	1.0	7.7	8.1	5.8	0.14	0.43	1.1	150.0	450.0	36	150
RGW_517PS0078	19	0.0350	0.7	5.8	9.0	7.3	0.21	0.32	1.2	92.0	1000.0	448	150
RGW_514CE0555	63	0.0580	0.3	2.7	8.2	1.3	0.24	0.27	1.2	250.0	1000.0	2	150
RGW_504PS0019	199	0.0060	0.8	7.9	10.2	35.1	0.32	0.13	1.1	22.0	40.0	4688	150
RGW_504CE0657	1	0.0110	0.5	6.1	16.4	7.1	0.59	0.37	1.4	64.0	250.0	5000	150
RGW_504PS0051	74	0.0210	1.3	22.2	17.1	23.9	0.13	0.30	1.2	55.0	185.0	4579	250
RGW_504PS0371	161	0.0100	1.0	14.6	18.2	40.6	0.58	0.28	1.1	24.0	80.0	4499	250
RGW_507PS0142	196	0.0130	1.5	21.2	16.3	17.2	0.24	0.41	1.3	85.0	250.0	295	250
RGW_508BERPRK	292	0.0110	1.4	12.4	10.0	22.2	0.38	0.26	1.0	95.0	5000.0	468	250
RGW_504DCFRxx	69	0.0360	1.5	8.1	6.0	5.9	0.49	0.34	1.1	250.0	5000.0	23	150
RGW_504WE0527	68	0.0290	1.7	17.8	10.4	7.2	0.09	0.10	1.1	250.0	2500.0	24	250
RGW_509CE0305	285	0.0210	1.0	19.6	22.3	15.8	0.48	0.31	1.2	80.0	192.0	98	250
RGW_509PS0334	302	0.0190	1.8	18.6	10.6	19.8	0.15	0.30	1.1	90.0	380.0	94	250
WS_0	77	0.0040	0.6	6.0	10.0	6.6	0.03	0.01	1.8	90.0	5000.0	19	250
WS_1	93	0.0030	0.8	7.4	9.4	280.5	0.24	0.18	1.1	2.8	22.6	65	150
WS_3	33	0.0290	0.2	3.2	14.5	7.0	0.04	0.02	1.1	32.0	128.0	670	250
WS_4	100	0.0010	1.1	11.1	10.1	69.2	0.12	0.32	1.4	16.0	45.0	731	250
WS_5	69	0.0030	0.5	8.0	16.1	89.3	0.45	0.20	1.5	5.6	32.0	401	150
WS_7	57	0.0030	1.0	12.0	11.6	8.1	0.16	0.11	1.1	128.0	200.0	27	150
WS_9	10	0.0170	0.6	4.2	6.9	4.8	0.33	0.28	1.1	128.0	5000.0	23	150
WS_10	69	0.0038	0.7	12.1	18.1	29.7	0.28	0.11	1.3	22.6	45.0	466	150
WS_11	32	0.0140	1.1	8.1	7.5	5.4	0.23	0.10	1.1	200.0	5000.0	5	150
WS_12	25	0.0090	0.9	7.4	8.8	9.4	0.23	0.15	1.1	90.0	200.0	56	150
WS_13	100	0.0040	1.0	8.3	8.2	62.8	0.29	0.12	1.3	16.0	45.0	580	150
WS_14	83	0.0160	0.8	13.2	15.6	37.3	0.27	0.26	1.3	22.6	200.0	64	150
WS_16	6	0.0170	0.7	4.4	3.6	7.3	0.28	0.25	1.3	90.0	1000.0	2	150
WS_17	10	0.0050	0.4	5.4	13.2	72.9	0.32	0.30	1.4	5.6	64.0	144	150
WS_18	6	0.0140	0.6	4.3	7.4	104.2	0.22	0.23	1.1	5.6	22.6	866	150
WS_20	69	0.0000	1.2	7.1	6.0	588.6	0.22	0.22	1.1	2.0	2.0	4375	150
WS_514PS0084	7	0.0000	0.5	4.0	7.9	51.0	0.41	0.78	1.1	10.0	1000.0	3842	150
WS_515PS0490	30	0.0010	1.0	6.7	6.7	515.0	0.20	0.06	1.1	2.0	2.0	4688	150
WS_520PS0202	25	0.0010	1.0	8.4	8.7	480.0	0.23	0.29	1.2	2.0	2.0	5000	150
WS_511CE0663	35	0.0120	1.6	7.6	4.9	815.0	0.23	0.13	1.2	2.0	250.0	1922	150

Table S4 (cont'd). Reach-scale data for all sites used in geomorphic classification (cont'd).

	Ac	s	d	w	w/d	d/D50	CVd	CVw	k	D50	D84	Cv	Ls
WS_514CE0523	7	0.012	0.7	4.3	7.6	325.0	0.29	0.21	1.2	2	16	297	150
WS_519CE0019	22	0.007	0.7	4.3	6.6	340.0	0.26	0.11	1.3	2	2	5000	150
WS_519CE0363	9	0.014	1.0	5.1	5.1	70.0	0.22	0.27	1.4	14	27	1197	150
WS_519CE0531	7	0.006	1.0	2.7	3.2	500.0	0.74	0.33	1.7	2	2	4375	150
WS_505PS0110	31	0.029	1.2	7.8	7.1	1.2	0.40	0.21	1.2	1000	5000	18	150
WS_506PS0003	16	0.030	1.0	5.8	7.7	4.2	0.70	0.32	1.2	245	5000	28	150
WS_506PS0062	11	0.047	0.6	5.1	8.8	7.5	0.15	0.18	1.1	80	350	15	150
WS_524SHA907	14	0.055	2.7	11.5	4.9	53.0	0.42	0.45	1.2	50	5000	11	250
WS_521LCCBSR	6	0.050	0.5	7.0	13.5	7.2	0.12	0.16	1.0	74	1000	17	150
WS_508SHA910	84	0.015	0.9	22.1	23.8	21.6	0.16	0.28	1.6	43	110	3066	250
WS_508SHA911	89	0.010	2.3	17.3	11.1	97.5	0.76	0.43	1.1	24	55	3279	250
WS_508SHA912	153	0.010	1.6	17.0	13.4	42.6	0.49	0.18	1.1	38	72	3777	250
WS_511PS0401	55	0.030	2.6	8.8	3.4	1285.0	0.07	0.15	1.2	2	13	4175	150
WS_514CE0171	56	0.016	1.8	14.3	8.2	28.0	0.15	0.15	1.2	64	250	2088	250
WS_519CE0211	86	0.006	1.0	7.5	7.7	515.0	0.26	0.17	1.1	2	2	3292	150
WS_505PS0174	50	0.018	1.5	11.3	8.1	3.3	0.20	0.21	1.2	445	5000	50	250
WS_519PS0340	48	0.009	0.7	6.7	10.3	335.0	0.29	0.29	1.3	2	90	2245	150
WS_526PS0764	88	0.085	1.3	11.0	8.6	1.3	0.17	0.40	1.1	1000	2500	647	250